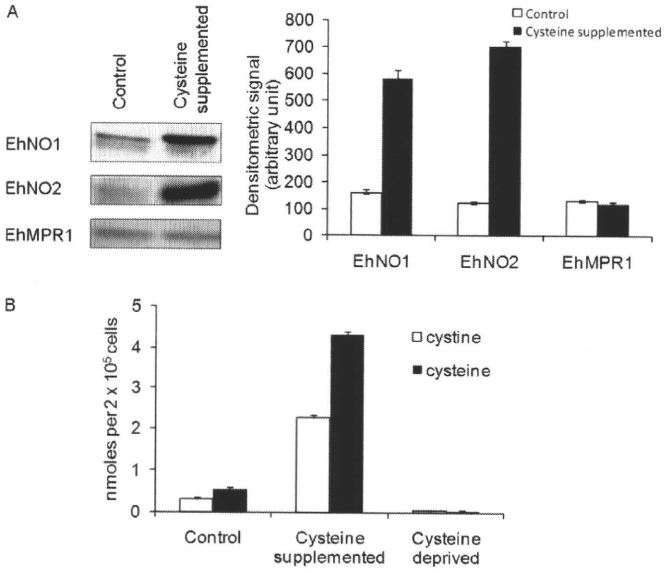

FIGURE 2. **Effects of extracellular L-cysteine concentrations on the amount of EhNO isotypes and intracellular L-cystine/L-cysteine concentrations.** *A*, an immunoblot analysis of EhNO1 and -2 is shown. After trophozoites were cultured under normal or L-cysteine-supplemented conditions for 48 h, ~15 μg of total cell lysate was electrophoresed on a 12% SDS-PAGE gel and subjected to an immunoblot assay with antibodies raised against EhNO1, EhNO2, or EhMPR1 as a control. The densitometric quantification of the reacted bands, shown in the *right graph*, was performed by Scion Image software, and the level of EhNO1, EhNO2, and EhMPR1 proteins was expressed in arbitrary units. *Error bars* represent the S.E. of three independent experiments. *B*, shown is intracellular L-cystine/cysteine concentrations under normal, L-cysteine-supplemented, and deprived conditions. L-Cystine/cysteine concentrations of the trophozoites cultivated for 48 h under the indicated conditions were analyzed by CE-MS. *Error bars* represent the S.E. of three independent experiments.

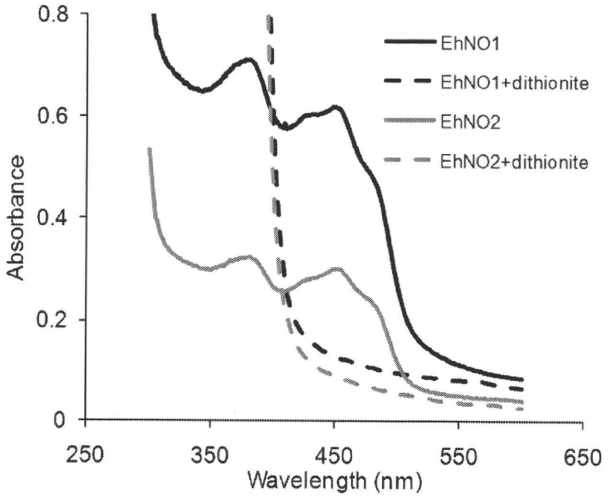

FIGURE 3. **Absorption spectra of rEhNO1 and rEhNO2 proteins.** UV-visible absorption spectra of rEhNO1 (400 μg of protein) and rEhNO2 (200 μg) under non-reducing (*solid lines*) and sodium dithionite-reducing conditions (*broken lines*) are shown. The samples were reduced with a 10-fold molar excess of sodium dithionite.

7-fold when cultured in the presence of 18 mM L-cysteine for 48 h compared with the control condition (8 mM L-cysteine), whereas it was down-regulated by 4-fold when cultured in the absence of L-cysteine. In contrast, the level of EhNO1 remained unchanged in either the presence or absence of L-cysteine.

Expression of EhNO Proteins under L-Cysteine-supplemented and -deprived Conditions—To confirm the changes of *EhNO* transcripts determined by the transcriptomic and real-time PCR analyses, we also examined EhNO expression at the protein level under L-cysteine-supplemented conditions. Immunoblot analysis using anti-rEhNO2 antibody showed that EhNO2 was induced by 6-fold when *E. histolytica* cultures were supplemented with L-cysteine (Fig. 2*A*). Although the RT-PCR results indicated that EhNO1 was not up-regulated under this condition, the protein recognized by anti-EhNO1 antibody was also found to be induced by 3.5-fold. Because anti-EhNO1 and anti-EhNO2 antibodies exhibited cross-reactivity (data not shown), the increased signal of the band recognized by anti-EhNO1 antibody was likely due to cross-reactivity with EhNO2. Alternatively, the level of EhNO1 may have increased by post-transcriptional mechanisms.

Changes in Intracellular L-Cysteine/Cystine Concentrations under L-Cysteine-supplemented and -deprived Conditions—To examine changes in intracellular L-cysteine and L-cystine concentrations caused by L-cysteine supplementation and deprivation, we quantitated their levels using a CE-MS-based approach in trophozoites maintained under normal (8 mM L-cysteine), enriched (18 mM L-cysteine), or deprived conditions. Under normal conditions, the L-cysteine to L-cystine ratio (1.70 ± 0.08) was deviated toward the reduced status. Upon L-cysteine supplementation, the intracellular levels of L-cysteine and L-cystine increased 8.1- and 7.3-fold, respectively, whereas under L-cysteine deprivation, both L-cysteine and L-cystine decreased to undetectable levels (Fig. 2*B*). Under L-cysteine-enriched conditions, the L-cysteine to L-cystine ratio (1.90 ± 0.14) slightly shifted toward the more reduced status (p = 0.031). Because several systems regulate the cellular redox reactions and electrochemical potential of the cell, the observed changes in the L-cysteine/cystine ratio were considered small. Taken together, these data clearly showed that although the extracellular L-cysteine concentration largely affects intracellular L-cysteine/L-cystine levels, its redox equilibrium is not severely affected. Furthermore, it appeared that a significant proportion of the L-cysteine incorporated into the cell was oxidized to L-cystine, which is supported by a previous finding (44). Alternatively, extracellular L-cysteine may be oxidized before uptake and reduced to L-cysteine intracellularly.

Expression and Purification of Recombinant EhNO Isotypes—To determine the biochemical properties of the two EhNO isoenzymes, recombinant proteins were first produced in *E. coli*. SDS-PAGE of the purified rEhNO1 and -2 proteins showed apparently single homogenous bands with molecular weights of 52.2 and 51.9 kDa, respectively, under reducing conditions (supplemental Fig. S3). The observed mobilities of rEhNO1 and -2 were consistent with the predicted sizes of the monomeric EhNO proteins with an extra 3.0-kDa histidine tag added at the amino terminus. The purity of the rEhNOs was estimated to be greater than 95% as judged by densitometric scanning of the stained gel. The rEhNO proteins were stable and retained their full activity for at least 3 months when stored in 10–15% glycerol at -30 or −80 °C.

Prosthetic Groups of rEhNOs—The UV-visible spectra of the purified rEhNOs showed absorbance maxima at 484, 450, 430, 378, and 280 nm (Fig. 3), which are characteristic of iron sulfur

flavoproteins (45). The dithionite-reduced rEhNOs showed, in contrast, a relatively featureless spectrum, with the increased absorbance at shorter wavelengths attributable to dithionite. Denaturation of the rEhNOs by boiling resulted in the release of flavin, indicating that it formed a non-covalent association with the protein. The fluorescence intensity of the free flavin at pH 2.6 was ~4-fold higher than that at pH 7.7 (data not shown). This indicates that FAD, rather than FMN, formed the prosthetic group in rEhNOs. It was calculated that 1.13 ± 0.32 mol of FAD (ϵ of FAD at 450 nm = 11.4×10^3 M^{-1} cm^{-1}) is associated per molecule of rEhNO1, whereas 0.89 ± 0.21 mol of FAD bound per molecule of rEhNO2. The iron analysis using the *O*-phenanthroline method indicated that rEhNO1 contained 7.8 ± 0.62 irons per molecule of rEhNO1, whereas rEhNO2 contained 7.4 ± 0.71 irons per molecule of rEhNO2. These results indicate that two [4Fe-4S] clusters are present per subunit, which is consistent with the $CX_2CX_4CX_3CP$ and $CX_3CX_3CX_3C$ motifs present in EhNO1 and -2. These data together with the stability of the enzymatic activity of rEhNOs also support the premise that rEhNOs retain most, if not all, of the features of the native EhNOs.

Kinetics Properties of rEhNO—The rEhNOs were devoid of glutamate synthase and glutamate dehydrogenase activity in both directions at either pH 7.5 or 9.5. However, both proteins oxidized NADPH and transferred electrons to several alternative electron acceptors, including INT, ferricyanide, and menadione (Table 1). In the presence of NADPH, the reduction rate of INT by rEhNO1 (specific activity 19.42 ± 3.25 μmol min^{-1} mg^{-1}) was >30-fold higher than that by rEhNO2 (0.62 ± 0.10 μmol min^{-1} mg^{-1}), whereas rEhNO2 showed a 2.8-fold higher ferricyanide reducing activity (86.64 ± 8.33 μmol min^{-1} mg^{-1}) than rEhNO1 (31.50 ± 6.21 μmol min^{-1} mg^{-1}). The menadione-reducing activities of rEhNO1 and -2 were comparable (2.48 ± 0.39 and 2.25 ± 0.41 μmol min^{-1} mg^{-1}, respectively). Both rEhNO1 and -2 were highly specific toward NADPH and did not reduce the above-tested electron acceptors with NADH as the electron donor. In the NADPH:flavin oxidoreductase reaction under aerobic conditions, rEhNO1 and -2 produced H_2O_2 at comparable levels (Table 1). Significantly, the two enzymes were also capable of reducing the anti-amebic drug metronidazole and the herbicide paraquat.

In addition to these properties, rEhNO1 and -2 could catalyze the reduction of disulfides, such as L-cystine, which was also dependent on NADPH. The K_m and k_{cat}/K_m values of rEhNO1 and -2 for L-cystine and NADPH were significantly different (Table 2). At substrate-saturating concentrations, the K_m values of rEhNO1 for L-cystine and L-NADPH were 3.3- and 2.3-fold higher, respectively, than those of rEhNO2. The k_{cat}/K_m value of rEhNO2 for L-cystine (measured at saturating concentrations of NADPH) was ~4-fold higher than that of rEhNO1. The addition of *N*-ethylmaleimide, which is commonly used to inhibit sulfydryl-dependent reactions, inhibited the disulfide reducing activities of both rEhNO1 and rEhNO2 (0.5 mM *N*-ethylmaleimide caused 50% inhibition), whereas the presence of up to 5 mM *N*-ethylmaleimide had no effect on the reduction of INT. These results indicate that the two EhNOs contain thiol(s) groups that are involved in disulfide reduction but are not required for their observed oxidoreductase activity (46, 47).

We also found that rEhNO1 and -2 catalyzed the reduction of ferric to ferrous ion. In the presence of NADPH, the reduction rate of Fe(III) by rEhNO1 (k_{cat}/K_m 15.1 ± 3.20 min^{-1} μM^{-1}) was ~116-fold higher than that by rEhNO2 (k_{cait}/K_m 0.12 ± 0.01 min^{-1} μM^{-1}) (Table 2). In addition, both rEhNOs also acted as ferredoxin:$NADP^+$ reductases capable of catalyzing the reduction of $NADP^+$ to NADPH through the utilization of the electrons provided by reduced ferredoxin, although the observed activity of EhNO1 was again higher (7.8-fold) than that of EhNO2. These data suggest that EhNO1 is mainly involved in the reduction of ferric ion and ferrodoxin:$NADP^+$, whereas EhNO2 primarily catalyzes the reduction of L-cystine. The uncatalyzed reaction rate (without enzyme) of each reaction was as follows: 22.5 ± 2.4 pmol/min, INT; 250 ± 32 pmol/min, ferricyanide; 29.2 ± 6.1 pmol/min, menadione; 307 ± 66 pmol/min, paraquat; 22.5 ± 7.8 pmol/min, cystine; 28.9 ± 6.9 pmol/min, ferric ammonium citrate; 6.16 ± 2.7 pmol/min, ferredoxin.

Binary Complexes of EhNO1/2 with Ferredoxins—To examine whether electron transfer between reduced ferredoxin and $NADP^+$ by EhNO1 was dependent on the physical interaction between these two proteins (48), as reported for the spinach leaf redox couple (36), we investigated whether EhNO1 and -2

TABLE 1
Specific activity of purified EhNO1 and EhNO2 with various electron acceptors
Values are expressed as the means ± S.D. of three independent experiments as described under "Experimental Procedures"

Substrate	Specific activity	
	rEhNO1	rEhNO2
	μmol/min/mg	
INT	19.42 ± 3.25	0.62 ± 0.10
Ferricyanide	31.50 ± 6.21	86.64 ± 8.33
Menadione	2.48 ± 0.39	2.25 ± 0.41
Metronidazole	1.75 ± 0.42	1.41 ± 0.46
Paraquat	19.73 ± 4.23	10.60 ± 2.12
Oxygen	8.31 ± 2.12	3.42 ± 0.81

TABLE 2
Kinetic parameters for cystine, ferric, and ferredoxin $NADP^+$ reductase reactions catalyzed by EhNO1 and EhNO2
Values are expressed as the means ± S.D. of three independent experiments.

Substrate	rEhNO1				rEhNO2			
	K_m	V_{max}	k_{cat}	k_{cat}/K_m	K_m	V_{max}	k_{cat}	k_{cat}/K_m
	μM	*μmol/min/mg*	min^{-1}	$min^{-1} \cdot \mu M^{-1}$	*μM*	*μmol/min/mg*	min^{-1}	$min^{-1} \cdot \mu M^{-1}$
Cystine	910 ± 20	0.88 ± 0.06	45.86 ± 7.52	0.05 ± 0.01	276 ± 23	1.15 ± 0.17	59.36 ± 3.81	0.22 ± 0.13
NADPH (cystine)	9.2 ± 2.1	1.70 ± 0.13	88.38 ± 5.83	9.61 ± 1.34	4.2 ± 0.8	1.33 ± 0.43	68.62 ± 5.40	16.33 ± 2.12
Fe(III) citrate	31.3 ± 3.4	9.10 ± 2.51	471.2 ± 17.5	15.1 ± 3.20	98.4 ± 4.5	0.26 ± 0.09	12.18 ± 2.81	0.12 ± 0.01
NADPH (ferric)	70.3 ± 4.9	10.12 ± 3.16	526.6 ± 21.2	7.49 ± 2.12	66.7 ± 8.3	0.72 ± 0.31	37.06 ± 6.28	0.56 ± 0.23
Ferredoxin	0.16 ± 0.05	2.28 ± 0.46	118.8 ± 7.4	742.5 ± 34.1	0.23 ± 0.07	0.43 ± 0.18	21.71 ± 4.51	94.39 ± 8.91

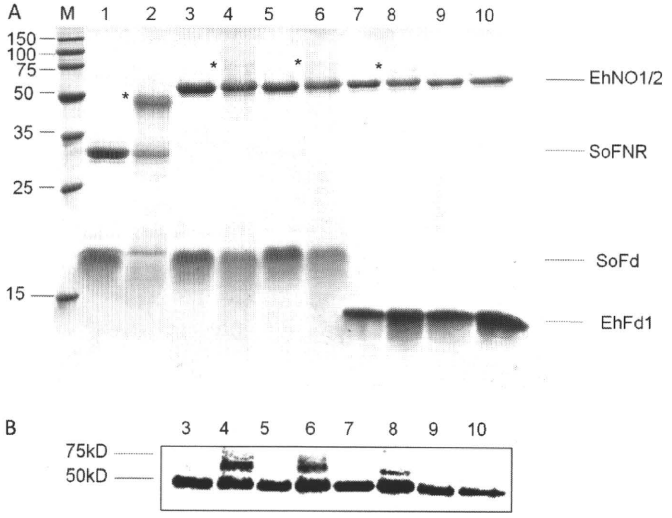

FIGURE 4. ***In vitro* interactions of EhNO with ferredoxin.** *A*, SDS-PAGE analysis of the complex of EhNO and ferredoxin is shown. Protein mixtures were incubated for 30 min with (*even lane numbers*) and without (*odd lane numbers*) 5 mM carbodiimide, electrophoresed on a 15% SDS-PAGE gel under reducing conditions, and then stained with Coomassie Brilliant Blue R250. The examined protein mixtures were as follows: *lanes 1* and *2*, spinach (*S. oleracea*) ferredoxin:NADP$^+$ reductase (*SoFNR*) + spinach ferredoxin (*SoFd*); *lanes 3* and *4*, *EhNO1*+*SoFd*; *lanes 5* and *6*, *EhNO2*+*SoFd*; *lanes 7* and *8*, *EhNO1*+*EhFd1*; *lanes 9* and *10*, *EhNO2*+*EhFd1*. Protein bands corresponding to the cross-linked proteins are indicated by an *asterisk*. The positions of the purified proteins are indicated on the *right side of the gel*. *B*, shown is an immunoblot analysis of the cross-linked samples using an anti-His antibody.

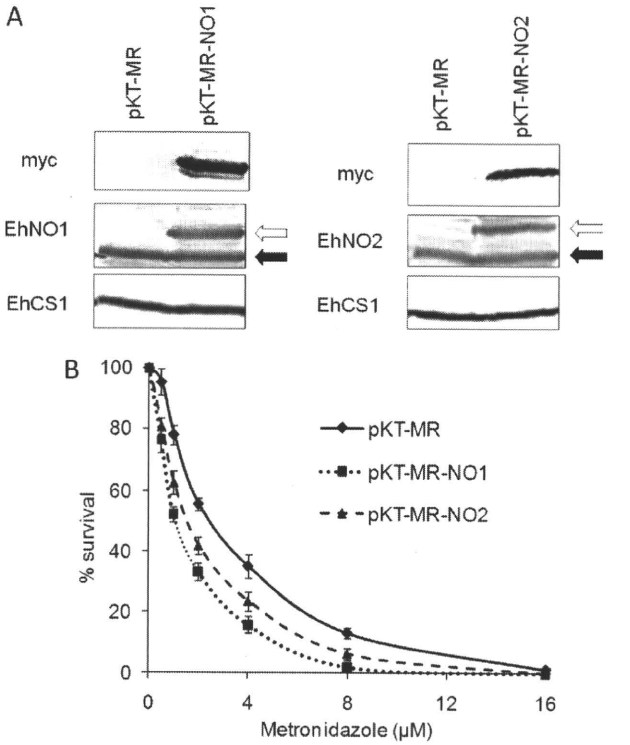

FIGURE 5. **Changes in the sensitivity of *E. histolytica* to metronidazole by overexpression of EhNOs.** *A*, shown is an immunoblot analysis of EhNOs in the transformants expressing Myc-tagged EhNO1 and -2. Approximately 40 μg of total lysate from the pKT-MR (control), EhNO1 (*pKT-MR-NO1*), and EhNO2 (*pKT-MR-NO2*)-overexpressing transformants was electrophoresed on a SDS-PAGE gel under reducing conditions and subjected to immunoblot analysis using anti-EhNO1, anti-EhNO2, anti-Myc, and anti-EhCS1 (*control*) antibodies. *Black* and *white arrows* indicate endogenous and Myc-tagged EhNO1 and -2, respectively. *B*, susceptibility of transformed trophozoites to metronidazole is shown. Trophozoites (10^4 cells/ml) were cultivated in the presence of 0–16 μM metronidazole for 48 h, and the number of viable cells was then counted. The percentages of living cells are shown relative to those of unexposed control cells. *Error bars* represent the S.E. of five independent experiments.

physically interacted with homologous and heterologous (*Spinacia oleracea*) ferredoxin (SoFd) using a carbodiimide-promoted cross-linking (50). We first cloned and purified a representative [3Fe4S] ferredoxin found in the *E. histolytica* genome data base (EhFd1; TIGR ID 128.m00136). For the assay, rEhNO1 and -2 were mixed with either purified EhFd1 or SoFd, cross-linked, and then analyzed by SDS-PAGE (Fig. 4*A*). It was observed that both rEhNO1 and -2 formed a complex with spinach ferredoxin, as shown by the appearance of a large 60-kDa band in the gel and more easily observed in the Western blot analysis using an anti-histidine antibody (Fig. 4*B*, *lanes 4* and *6*). However, only EhNO1 formed a complex with *E. histolytica* ferredoxin (EhFd1) (Fig. 4, *A* and *B*, *lanes 8* and *10*).

Cellular Distribution of EhNO—We also examined the cellular distribution of EhNO1 and -2 in trophozoites. The immunofluorescence imaging using antiserum raised against the corresponding recombinant protein revealed that the two isotypes were distributed throughout the cytosol (data not shown). We also verified the localization of EhNOs by immunoblotting using lysates produced by a Dounce glass homogenizer followed by sonication and centrifugation at 100,000 × *g* at 4 °C for 1 h. Both EhNO1 and -2 fractionated into the soluble fraction (data not shown).

Increased Metronidazole Sensitivity by EhNO Overexpression—To confirm that EhNO is the target of metronidazole in *E. histolytica*, stable transformants that overexpressed Myc-tagged EhNO1 or 2 were generated. Both the transformants expressing Myc-tagged EhNO1 or EhNO2 expressed ~2-fold higher levels of the corresponding enzymes than the control (Fig. 5*A*) and were more sensitive to metronidazole. The 50% growth inhibitory concentrations (IC_{50}) of metronidazole for the Myc-EhNO1- and Myc-EhNO2-overexpressing transformants were 1.03 ± 0.05 and 1.42 ± 0.12 μM, respectively (Fig. 5*B*), whereas the control showed an IC_{50} of 2.24 ± 0.33 μM.

DISCUSSION

In the present study we demonstrated novel enzymatic reactions catalyzed by a new class of FAD- and 2[4Fe-4S]-containing NADPH-dependent oxidoreductases from *E. histolytica*, which had been initially discovered by virtue of tightly regulated gene expression in correlation with L-cysteine concentrations. Although the two EhNOs characterized in this study had been annotated before this study based on their high degree of homology with GOGAT β subunit and β subunit-like genes from a variety of organisms, their biochemical function was unknown. The fact that the two EhNOs shared significant similarity with homologs from archaeal organisms raised the question of whether they represented a prototype GOGAT protein, similar to the β subunit protein from *Pyrococcus*, which was reported to possess NADPH-dependent GOGAT activity and be capable of both glutamine and ammonia-dependent synthesis in the absence of the α subunit (7). However, we were unable to observe glutamate synthase activity of the EhNOs under similar conditions used for the *Pyrococcus* glutamate synthase. Fur-

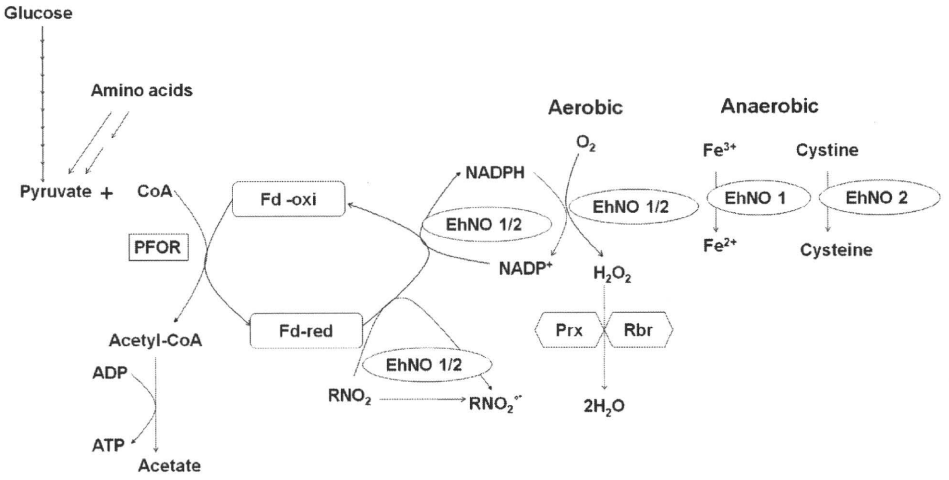

FIGURE 6. **Proposed *in vivo* reactions catalyzed by EhNO1 and -2.** *PFOR*, pyruvate:ferredoxin oxidoreductase; *Fd-red* and *Fd-oxi*, reduced and oxidized form of ferredoxin; *Prx*, peroxiredoxin; *Rbr*, rubrerythrin; RNO_2/$RNO_2^{\cdot}$, metronidazole/reduced metronidazole.

thermore, the expression of the GOGAT β subunit failed to restore glutamate auxotrophy in an *E. coli* GOGAT α subunit-deficient strain (5, 51). In addition, it was somewhat puzzling how the *Pyrococcus* GOGAT β subunit functioned in substrate binding and catalysis without the α subunit, which has been shown to be responsible for substrate recognition (52). Thus, it was thought that the EhNO β subunit-like proteins may be involved in reactions other than glutamate synthesis.

The physiological roles of EhNO1 and EhNO2 have not been unequivocally demonstrated because our attempt to repress EhNO expression by gene silencing (53) failed (data not shown), and gene knock-out has not been accomplished in *E. histolytica*. Nevertheless, our present enzymological characterization revealed the physiological significance of the presence of the two isotypes of EhNOs. EhNO2 appears to play an important role in the reduction of cystine to L-cysteine. Because L-cysteine is partially present in the oxidized form inside cells (CE-MS analysis, Fig. 2*B*), L-cystine reduction is necessary before the utilization of L-cysteine, which has been implicated in the attachment to matrix, elongation, motility, growth, and anti-oxidative defense (35, 54, 55). Transcriptomic analysis demonstrated that the transcription of EhNO2, but not EhNO1, is tightly regulated by extracellular L-cysteine concentrations. Furthermore, the measured kinetic parameters indicate that EhNO2 possesses 4-fold higher L-cystine reduction efficiency than EhNO1.

The acquisition of iron and subsequent assimilation into cellular proteins are ubiquitously essential for life. However, at physiological pH under aerobic conditions, iron is present as Fe^{3+} hydroxides and oxyhydroxides or in a complex with ferric-specific chelators, *e.g.* siderophores (56). Subsequent reduction of complexed Fe^{3+} is accomplished by ferric reductases using NAD(P)H as the electron donor (57), with the resulting Fe^{2+} being subsequently released and incorporated into iron-containing proteins (58). We showed that rEhNO1 catalyzes the reduction of ferric ion >100-fold more efficiently than rEhNO2 (Table 2), suggesting that EhNO1 is mainly involved in ferric reduction. We also confirmed that EhNO1 functions as a ferredoxin:$NADP^+$ reductase, similar to the recently reported ferric reductase from *Pseudomonas putida* (59), by catalyzing reversible electron transfer between one molecule of $NADP^+$/NADPH and two molecules of ferredoxin. *In vitro* cross-linking of the two EhNOs with ferredoxin indicate that only EhNO1 forms a stable complex with *E. histolytica* ferredoxin (EhFd1), whereas both EhNO1 and EhNO2 physically interact with spinach ferredoxin (Fig. 4*B*), indicating that the specificity toward ferredoxin differs between these two proteins. The *E. histolytica* genome encodes four types of ferredoxins which are highly divergent at the primary sequence level and also in the Fe-S clusters. We, therefore, hypothesize that EhNO2 interacts with a ferredoxin(s) other than EhFd1 in *E. histolytica*, a speculation that is supported by the observed differential binding of photosynthetic and non-photosynthetic maize ferredoxins to root *Zea mays* ferredoxin:$NADP^+$ reductase (60).

E. histolytica is anaerobic/microaerophilic and possesses highly degenerated mitochondria that are incapable of oxidative phosphorylation and ATP generation. A crucial step in energy production via glycolysis and fermentation in *E. histolytica* involves the decarboxylation of pyruvate to acetyl CoA that is catalyzed by pyruvate:ferredoxin oxidoreductase (61). Concomitant with the decarboxylation of pyruvate, an electron is transferred to oxidized ferredoxin. Generally, reduced ferredoxin subsequently donates an electron to NAD(P) by the action of ferredoxin:NADP reductase, which serves to regenerate the intracellular pools of NAD(P)H and oxidized ferredoxin. However, as the *Entamoeba* genome does not contain an ferredoxin:NADP reductase homolog, it was unclear how NAD(P)H was regenerated. Our enzymological study indicates that EhNOs, and EhNO1 in particular, function as ferredoxin:NADP reductases and are involved in the regeneration of NADPH and oxidized ferredoxin required for continuous energy production.

As stated above, *E. histolytica* possesses highly divergent mitochondria (62) and lacks a functional tricarboxylic acid cycle, cytochromes, and a conventional respiratory electron transport chain terminating in the reduction of oxygen to water. However, amebae can still tolerate up to 5% of oxygen in the gas phase (63, 64) and consume oxygen (65). As shown here, EhNOs are flavoproteins containing 1 mol of FAD as a prosthetic group per mol of enzyme. During the NADPH:flavin oxidoreductase reaction, NADPH binds to EhNOs, and two electrons are transferred to FAD to yield $FADH_2$, which is immediately dissociated from the enzyme (66). Under aerobic conditions, $FADH_2$ is rapidly oxidized by molecular oxygen to yield H_2O_2 and FAD (67). As *E. histolytica* amebae do not produce detectable amounts of H_2O_2 (27), it is possible that H_2O_2 is further converted to water by peroxiredoxin (68) and rubrerythrin (69) to overcome oxidative stress. Under anaero-

bic conditions, EhNO1 catalyzes ferric ion reduction, whereas EhNO2 catalyzes cystine reduction. Based on the demonstrated reactions catalyzed by the two EhNOs, we have proposed functional roles for these two proteins in *E. histolytica* that are summarized in Fig. 6.

Metronidazole is a prodrug currently used to treat a number of microbial infections, and its activation requires intracellular reduction to produce cytotoxic short-lived radicals and other reactive species (70). *Entamoeba* electron transport proteins, which have been reported to provide the source of electrons for the reductive activation of metronidazole, include ferredoxin (71), thioredoxin reductase (72), and nitroreductase (49). We demonstrated that both EhNO1 and -2 catalyze metronidazole reduction *in vitro* (Table 1), and their overexpression confers increased sensitivity to this drug (Fig. 5*B*). This finding suggests that in addition to ferredoxin (71), pyruvate:ferredoxin oxidoreductase (71), thioredoxin (72), and nitroreductase (49), EhNO1 and -2 are also involved in metronidazole activation in *E. histolytica*.

In conclusion, we have demonstrated for the first time that two novel NADPH-dependent GOGAT small subunit-like proteins of *E. histolytica* function, at least *in vitro*, as cystine/ferric/ferredoxin:$NADP^+$ reductase. We propose that they play a role in maintaining intracellular redox potential and may be responsible for metronidazole activation in this parasite. The physiological substrates and biological roles of the majority of oxidoreductases discovered by genome mining remain largely unknown. Vigorous attempts to discover the substrates and functions of individual oxidoreductases should unveil novel cellular metabolic processes in pathogens and cancer cells that may lead to the development of new chemotherapeutics.

Acknowledgments—We thank Kumiko Nakada-Tsukui, Fumika Michi, Takashi Makiuchi, and all other members of our laboratory for technical assistance and valuable discussions.

REFERENCES

1. Ratti, S., Curti, B., Zanetti, G., and Galli, E. (1985) *J. Bacteriol.* **163,** 724–729
2. Rosenbaum, K., Jahnke, K., Curti, B., Hagen, W. R., Schnackerz, K. D., and Vanoni, M. A. (1998) *Biochemistry* **37,** 17598–17609
3. Tóth, A., Takács, M., Groma, G., Rákhely, G., and Kovács, K. L. (2008) *FEMS Microbiol. Lett.* **282,** 8–14
4. Vanoni, M. A., and Curti, B. (1999) *Cell Mol. Life Sci.* **55,** 617–638
5. Stutz, H. E., and Reid, S. J. (2004) *Biochim. Biophys. Acta* **1676,** 71–82
6. Saum, S. H., Sydow, J. F., Palm, P., Pfeiffer, F., Oesterhelt, D., and Müller, V. (2006) *J. Bacteriol.* **188,** 6808–6815
7. Jongsareejit, B., Rahman, R. N., Fujiwara, S., and Imanaka, T. (1997) *Mol. Gen. Genet.* **254,** 635–642
8. World Health Organization (1997) *WHO/PAHO/UNESCO Report: A consultation with experts on amebiasis. Mexico City, Mexico 28–29 January, 1997. Epidemiol. Bull* **18,** 13–14
9. Upcroft, P., and Upcroft, J. A. (2001) *Clin. Microbiol. Rev.* **14,** 150–164
10. Hoffman, J. S., and Cave, D. R. (2001) *Curr. Opin. Gastroenterol.* **17,** 30–34
11. World Health Organization (2007 March) *WHO Model List of Essential Medicines*, 15th Ed.
12. Müller, M. (1983) *Surgery* **93,** 165–171
13. Moreno, S. N., and Docampo, R. (1985) *Environ. Health Perspect.* **64,** 199–208
14. West, S. B., Wislocki, P. G., Fiorentini, K. M., Alvaro, R., Wolf, F. J., and Lu,, A. Y. (1982) *Chem. Biol. Interact.* **41,** 265–279
15. Ludlum, D. B., Colinas, R. J., Kirk, M. C., and Mehta, J. R. (1988) *Carcinogenesis* **9,** 593–596
16. Diamond, L. S., Harlow, D. R., and Cunnick, C. C. (1978) *Trans. R. Soc. Trop. Med. Hyg.* **72,** 431–432
17. Clark, C. G., and Diamond, L. S. (2002) *Clin. Microbiol. Rev.* **15,** 329–341
18. Thompson, J. D., Higgins, D. G., and Gibson, T. J. (1994) *Nucleic Acids Res.* **22,** 4673–4680
19. Leão-Helder, A. N., Krikken, A. M., Gellissen, G., van der Klei, I. J., Veenhuis, M., and Kiel, J. A. (2004) *FEBS Lett.* **577,** 491–495
20. Kumar, S., Tamura, K., Jakobsen, I. B., and Nei, M. (2001) *Bioinformatics* **17,** 1244–1245
21. Sambrook, J., and Russell, D. W. (2001) *Molecular Cloning: A Laboratory Manual*, 3rd Ed., Cold Spring Harbor Laboratory Press, Cold Spring Harbor, NY
22. Nozaki, T., Asai, T., Kobayashi, S., Ikegami, F., Noji, M., Saito, K., and Takeuchi, T.. (1998) *Mol. Biochem. Parasitol.* **97,** 33–44
23. Bradford, M. M. (1976) *Anal. Biochem.* **72,** 248–254
24. Faeder, E. J., and Siegel, L. M. (1973) *Anal. Biochem.* **53,** 332–336
25. Olson, J. W., Agar, J. N., Johnson, M. K., and Maier, R. J. (2000) *Biochemistry* **39,** 16213–16219
26. Chen, J. S., and Blanchard, D. K. (1979) *Anal. Biochem.* **93,** 216–222
27. Lo, H., and Reeves, R. E. (1980) *Mol. Biochem. Parasitol.* **2,** 23–30
28. Ichikawa, Y., Hiwatashi, A., Yamano, T., Kim, H. J., and Maruya, N. (1980) in *Flavins and Flavoproteins* (Yagi, K., and Yamano, T., eds) pp. 677–691, University Park Press, Baltimore, MD
29. Thurman, R. G., Ley, H. G., and Scholz, R. (1972) *Eur. J. Biochem.* **25,** 420–430
30. Soga, T., and Heiger, D. N. (2000) *Anal. Chem.* **72,** 1236–1241
31. Soga, T., Ohashi, Y., Ueno, Y., Naraoka, H., Tomita, M., and Nishioka, T. (2003) *J. Proteome Res.* **2,** 488–494
32. Soga, T., Baran, R., Suematsu, M., Ueno, Y., Ikeda, S., Sakurakawa, T., Kakazu, Y., Ishikawa, T., Robert, M., Nishioka, T., and Tomita, M. (2006) *J. Biol. Chem.* **281,** 16768–16776
33. Ohashi, Y., Hirayama, A., Ishikawa, T., Nakamura, S., Shimizu, K., Ueno, Y., Tomita, M., and Soga, T. (2008) *Mol. Biosyst.* **4,** 135–147
34. Nakada-Tsukui, K., Okada, H., Mitra, B. N., and Nozaki, T. (2009) *Cell. Microbiol.* **11,** 1471–1491
35. Nozaki, T., Asai, T., Sanchez, L. B., Kobayashi, S., Nakazawa, M., and Takeuchi, T. (1999) *J. Biol. Chem.* **274,** 32445–32452
36. Zanetti, G., Morelli, D., Ronchi, S., Negri, A., Aliverti, A., and Curti, B. (1988) *Biochemistry* **27,** 3753–3759
37. Tokoro, M., Asai, T., Kobayashi, S., Takeuchi, T., and Nozaki, T. (2003) *J. Biol. Chem.* **278,** 42717–42727
38. Nakada-Tsukui, K., Saito-Nakano, Y., Ali, V., and Nozaki, T. (2005) *Mol. Biol. Cell* **16,** 5294–5303
39. Srivastava, M., Ahmad, N., Gupta, S., and Mukhtar, H. (2001) *J. Biol. Chem.* **276,** 15481–15488
40. Loftus, B., Anderson, I., Davies, R., Alsmark, U. C., Samuelson, J., Amedeo, P., Roncaglia, P., Berriman, M., Hirt, R. P., Mann, B. J., Nozaki, T., Suh, B., Pop., M., Duchene, M., Ackers, J., Tannich, E., Leippe, M., Hofer, M., Bruchhaus, I., Willhoeft, U., Bhattacharya, A., Chillingworth, T., Churcher, C., Hance, Z., Harris, B., Harris, D., Jagels, K., Moule, S., Mungall, K., Ormond, D., Squares, R., Whitehead, S., Quail, M. A., Rabbinowitsch, E., Norbertczak, H., Price, C., Wang, Z., Guillén, N., Gilchrist, C., Stroup, S. E., Bhattacharya, S., Lohia, A., Foster, P. G., Sicheritz-Ponten, T., Weber, C., Singh, U., Mukherjee, C., El-Sayed, N. M., Petri, W. A., Jr, Clark, C. G., Embley, T. M., Barrell, B., Fraser, C. M., and Hall, N. (2005) *Nature* **433,** 865–868
41. Morandi, P., Valzasina, B., Colombo, C., Curti, B., and Vanoni, M. A. (2000) *Biochemistry* **39,** 727–735
42. Pelanda, R., Vanoni, M. A., Perego, M., Piubelli, L., Galizzi, A., Curti, B., and Zanetti, G. (1993) *J. Biol. Chem.* **268,** 3099–3106
43. Andersson, J. O., and Roger, A. J. (2002) *Eukaryot. Cell* **1,** 304–310
44. Gillin, F. D., and Diamond, L. S. (1981) *Exp. Parasitol.* **51,** 382–391
45. Latimer, M. T., Painter, M. H., and Ferry, J. G. (1996) *J. Biol. Chem.* **271,** 24023–24028
46. Fontecave, M., Eliasson, R., and Reichard, P. (1987) *J. Biol. Chem.* **262,** 12325–12331

47. Jablonski, E., and DeLuca, M. (1978) *Biochemistry* **17,** 672–678
48. Foust, G. P., Mayhew, S. G., and Massey, V. (1969) *J. Biol. Chem.* **244,** 964–970
49. Pal, D., Banerjee, S., Cui, J., Schwartz, A., Ghosh, S. K., and Samuelson, J. (2009) *Antimicrob. Agents Chemother.* **53,** 458–464
50. Zanetti, G., Aliverti, A., and Curti, B. (1984) *J. Biol. Chem.* **259,** 6153–6157
51. Deane, S. M., and Rawlings, D. E. (1996) *Gene* **177,** 261–263
52. Vanoni, M. A., Fischer, F., Ravasio, S., Verzotti, E., Edmondson, D. E., Hagen, W. R., Zanetti, G., and Curti, B. (1998) *Biochemistry* **37,** 1828–1838
53. Bracha, R., Nuchamowitz, Y., Anbar, M., and Mirelman, D. (2006) *PLoS Pathog.* **2,** e48
54. Gillin, F. D., and Diamond, L. S. (1981) *Exp. Parasitol.* **52,** 9–17
55. Gillin, F. D., and Diamond, L. S. (1980) *J. Protozool.* **27,** 474–478
56. Barchini, E., and Cowart, R. E. (1996) *Arch. Microbiol.* **166,** 51–57
57. Lesuisse, E., Crichton, R. R., and Labbe, P. (1990) *Biochim. Biophys. Acta* **1038,** 253–259
58. Guerinot, M. L. (1994) *Annu. Rev. Microbiol.* **48,** 743–772
59. Yeom, J., Jeon, C. O., Madsen, E. L., and Park, W. (2009) *J. Bacteriol.* **191,** 1472–1479
60. Onda, Y., Matsumura, T., Kimata-Ariga, Y., Sakakibara, H., Sugiyama, T., and Hase, T. (2000) *Plant Physiol.* **123,** 1037–1045
61. Kerscher, L., and Oesterhelt, D. (1982) *Trends Biol. Sci.* **7,** 371–374
62. Tovar, J., Fischer, A., and Clark, C. G. (1999) *Mol. Microbiol.* **32,** 1013–1021
63. Band, R. N., and Cirrito, H. (1979) *J. Protozool.* **26,** 282–286
64. Reeves, R. E. (1984) *Adv. Parasitol.* **23,** 105–142
65. Weinbach, E. C., and Diamond, L. S. (1974) *Exp. Parasitol.* **35,** 232–243
66. Inouye, S. (1994) *FEBS Lett.* **347,** 163–168
67. Gibson, Q. H., and Hastings, J. W. (1962) *Biochem. J.* **83,** 368–377
68. Bruchhaus, I., Richter, S., and Tannich, E. (1997) *Biochem. J.* **326,** 785–789
69. Maralikova, B., Ali, V., Nakada-Tsukui, K., Nozaki, T., van der Giezen, M., Henze, K., and Tovar, J. (2010) *Cell Microbiol.* **12,** 331–342
70. Goldman, P., Koch, R. L., Yeung, T. C., Chrystal, E. J., Beaulieu, B. B., Jr., McLafferty, M. A., and Sudlow, G. (1986) *Biochem. Pharmacol.* **35,** 43–51
71. Müller, M. (1986) *Biochem. Pharmacol.* **35,** 37–41
72. Leitsch, D., Kolarich, D., Wilson, I. B. H., Altmann, F., and Duchene, M. (2007) *PLoS Biol.* **5,** e211

EUKARYOTIC CELL, June 2010, p. 926–933
1535-9778/10/$12.00 doi:10.1128/EC.00011-10

Vol. 9, No. 6

Localization and Targeting of an Unusual Pyridine Nucleotide Transhydrogenase in *Entamoeba histolytica*▽

Mohammad Abu Yousuf,[1,2] Fumika Mi-ichi,[1] Kumiko Nakada-Tsukui,[1] and Tomoyoshi Nozaki[1]*

Department of Parasitology, National Institute of Infectious Diseases, Tokyo 162-8640, Japan,[1] and Department of Parasitology, Gunma University Graduate School of Medicine, 3-39-22 Showa-machi, Maebashi 371-8511, Japan[2]

Received 17 January 2010/Accepted 3 April 2010

Pyridine nucleotide transhydrogenase (PNT) catalyzes the direct transfer of a hydride-ion equivalent between NAD(H) and NADP(H) in bacteria and the mitochondria of eukaryotes. PNT was previously postulated to be localized to the highly divergent mitochondrion-related organelle, the mitosome, in the anaerobic/microaerophilic protozoan parasite *Entamoeba histolytica* based on the potential mitochondrion-targeting signal. However, our previous proteomic study of isolated phagosomes suggested that PNT is localized to organelles other than mitosomes. An immunofluorescence assay using anti-*E. histolytica* PNT (*Eh*PNT) antibody raised against the NADH-binding domain showed a distribution to the membrane of numerous vesicles/vacuoles, including lysosomes and phagosomes. The domain(s) required for the trafficking of PNT to vesicles/vacuoles was examined by using amoeba transformants expressing a series of carboxyl-terminally truncated PNTs fused with green fluorescent protein or a hemagglutinin tag. All truncated PNTs failed to reach vesicles/vacuoles and were retained in the endoplasmic reticulum. These data indicate that the putative targeting signal is not sufficient for the trafficking of PNT to the vesicular/vacuolar compartments and that full-length PNT is necessary for correct transport. PNT displayed a smear of >120 kDa on SDS-PAGE gels. PNGase F and tunicamycin treatment, chemical degradation of carbohydrates, and heat treatment of PNT suggested that the apparent aberrant mobility of PNT is likely attributable to its hydrophobic nature. PNT that is compartmentalized to the acidic compartments is unprecedented in eukaryotes and may possess a unique physiological role in *E. histolytica*.

Pyridine nucleotide transhydrogenase (PNT) participates in the bioenergetic processes of the cell. PNT generally resides on the cytoplasmic membranes of bacteria and the inner membrane of mammalian mitochondria (3, 16) and utilizes the electrochemical proton gradient across the membrane to drive NADPH formation from NADH (14, 15, 39) according to the reaction H^+out + NADH + $NADP^+ \leftrightarrow H^+$in + NAD^+ + NADPH, where "out" and "in" denote the cytosol and the matrix of the mitochondria, or the periplasmic space and the cytosol of bacteria, respectively.

PNT has been identified in several protozoan parasites, including *Entamoeba histolytica* (8, 51), *Eimeria tenella* (17, 47), *Mastigamoeba balamuthi* (11) *Plasmodium falciparum* (10), *Plasmodium yoelii* (6), and *Plasmodium berghei* (12). In general, PNT contains conserved structural units consisting of three domains, the NAD(H)-binding domain (domain I [dI]) and the NADP(H)-binding domain (domain III [dIII]), both of which face the matrix side of the eukaryotic mitochondria or the cytoplasmic side in bacteria, and the hydrophobic domain (domain II [dII]), containing 11 to 13 transmembrane regions. PNT from *E. tenella* and *E. histolytica* exists as a single polypeptide in an unusual configuration consisting of dIIb-dIII-dI-dIIa, with a 38-amino-acid-long linker region between dIII and dI (48).

E. histolytica, previously considered an "amitochondriate" protist, is currently considered to possess a mitochondrion-related organelle with reduced and divergent functions, the mitosome (1, 21, 23a, 26, 42). Our recent proteomic study of isolated mitosomes identified about 20 new constituents (26), together with four proteins previously demonstrated in *E. histolytica* mitosomes: Cpn60 (8, 19, 21, 42), Cpn10 (46), mitochondrial Hsp70 (2, 44), and mitochondrion carrier family (MCF) (ADP/ATP transporter) (7). Despite the early presumption of PNT being localized in mitosomes (8), based on the amino-terminal region rich in hydroxylated (five serines and threonines) and acidic (three glutamates) amino acids, which slightly resembles known mitochondrion- and hydrogenosome-targeting sequences (8, 35), PNT was not discovered in the mitosome proteome. We also doubted this premise because PNT was one of the major proteins identified in isolated phagosomes (32, 33). Thus, the intracellular localization and trafficking of PNT remain unknown.

In this report, we showed that *E. histolytica* PNT (*Eh*PNT) is localized to various vesicles and vacuoles, including lysosomes and phagosomes, using wild-type amoebae and antiserum raised against recombinant *Eh*PNT and an *E. histolytica* line expressing *Eh*PNT with a carboxyl-terminal hemagglutinin (HA) epitope tag and anti-HA antibody. We also showed that all domains of *Eh*PNT are required for its trafficking to the acidic compartment by using amoeba transformants expressing the HA tag or green fluorescent protein (GFP) fused with a region containing various domains of *Eh*PNT.

MATERIALS AND METHODS

Cells, cultures, and reagents. Trophozoites of *E. histolytica* strain HM-1:IMSS cl6 were maintained axenically in Diamond's BI-S-33 medium (9) at 35.5°C.

* Corresponding author. Mailing address: Department of Parasitology, National Institute of Infectious Diseases, 1-23-1 Toyama, Shinjuku, Tokyo 162-8640, Japan. Phone: 81 3 5285 1111, ext. 2600. Fax: 81 3 5285 1219. E-mail: nozaki@nih.go.jp.

▽ Published ahead of print on 9 April 2010.

Chinese hamster ovary (CHO) cells were maintained in F12 medium (Invitrogen, San Diego, CA) supplied with 10% fetal calf serum (Medical Biological Laboratory International, Woburn, MA) at 37°C with 5% CO_2. *Escherichia coli* strains DH5α and BL21(DE3) were purchased from Life Technologies (Tokyo, Japan) and Novagen (Madison, WI), respectively. LysoTracker Red DND-99 and CellTracker Orange CMTMR [5-(and-6)-(((4-chloromethyl)benzoyl)amino)tetramethylrhodamine] were purchased from Molecular Probes (Eugene, OR). All other chemicals of analytical grade were purchased from Sigma-Aldrich unless otherwise stated.

Plasmid construction. Standard techniques were used for routine DNA manipulation, subcloning, and plasmid construction as previously described (38). To produce *E. coli* recombinant proteins, a coding region corresponding to dI (amino acids [aa] 565 to 960) of *Eh*PNT (*Eh*PNTdI) was amplified from an *E. histolytica* cDNA library by using a pair of appropriate primers designed on the basis of the nucleotide sequences in the GenBank database (accession number L39933) (8), with BamHI and XhoI restriction enzyme sites. The sense and antisense primers were 5′-CGA**GGATCC**GATGTTATTTATTGGTATTCCAA AAG-3′ and 5′-CGTT**CTCGAG**TCATTCTTCTTCAGTTGAAAGA-3′, respectively, where boldface type indicates the BamHI or XhoI site. The PCR products were cloned into the BamHI- and XhoI-digested vector pET47b (Novagen, Madison, WI), and the resulting plasmid was designated pHisPNTdI. To generate vectors to express either full-length or truncated forms of *Eh*PNT fused to HA in the amoeba, a protein-coding region corresponding to full-length *Eh*PNT (GenBank accession number AAC41577) (aa 1 to 1083), the 14-aa amino-terminal region encompassing the putative targeting sequence (TS)+dIIb (aa 1 to 330), TS+dIIb+dIII (aa 1 to 525), TS+dIIb+dIII+linker (aa 1 to 564), and TS+dIIb+dIII+ linker+dI (aa 1 to 960) was amplified from an *E. histolytica* cDNA library by using a pair of appropriate primers and cloned into the BglII site of pEhExHA (29). The antisense primers were 5′-CGT**GGATCC**ATGAAA CATTTTCAACATTCTG-3′, 5′-CGT**GGATCC**GAATGATCTATTCATAGCT TTACAC-3′, 5′-CGT**GGATCC**TTCTTCATTTAATTCTTCAAATCCTTTC-3′, 5′-CGT**GGATCC**ATCTTCTGCAAGAACTTTTGTTGGA-3′, and 5′-CGT**GG ATCC**TTCTTCTTCAGTTGAAAGAGT-3′, respectively, where boldface type represents the BamHI site. The sense primer described above was used for these full-length or truncated forms of *Eh*PNT to express in the amoeba. To generate a plasmid to express GFP fused to the *Eh*PNT TS, a pair of oligonucleotides corresponding to the TS were generated, self-annealed, and cloned into the BglII site of pEhExGFP. The oligonucleotides were 5′-**GATCT**ATGAGCACAAGTT CTAGTATTGAAGAAGAAGTGTTCAATTATA-3′ and 5′-**GATCT**ATAATT GAACACTTCTTCTTCAATACTAGAACTTGTGCTCATA-3′, where boldface type represents the truncated BglII site. pEhExGFP was generated by the ligation of the GFP protein-coding region of pKT-MG (29) into the BglII-XhoI site of pEhEx (31). These constructs allowed the expression of PNT with the three tandem copies of the HA tag or GFP at the carboxyl terminus. The resulting plasmids were designated pPNTFL-HA, pTS/IIb-HA, pTS/IIb/III-HA, pTS/dIIb/dIII/L-HA, pTS/IIb/III/L/I-HA, and pPNTTS-GFP. The production of the Cpn60-HA transformant was previously described (26).

Amoeba transformation. Plasmids generated as described above were introduced into amoeba trophozoites by lipofection as previously described (30). Geneticin (Invitrogen, San Diego, CA) was added at a concentration of 1 μg/ml at 24 h after transfection, and the Geneticin concentration was gradually increased for approximately 2 weeks until it reached 10 μg/ml.

Recombinant protein production. pHisPNTdI was introduced into BL21(DE3) cells. The expression of the histidine-tagged *Eh*PNTdI protein was induced with 1 mM isopropyl-β-thiogalactoside at 37°C for 3 h. After harvesting and washing three times with phosphate-buffered saline (PBS) (pH 7.4), the bacteria were lysed in B-PER reagent (Pierce, Rockford, IL) containing Complete Mini EDTA-free protease inhibitor cocktail (Roche Diagnostic, Mannheim, Germany) and mixed with 1.0 ml of a 50% slurry of Ni^{2+}-nitrilotriacetic acid (NTA) His-Bind resin. The recombinant *Eh*PNTdI-bound resin was washed in a column three times with 25 ml of buffer A (50 mM NaH_2PO_4, 300 mM NaCl [pH 8.0]) containing 20 mM imidazole. Bound proteins were eluted with buffer A containing 1 M imidazole and dialyzed against PBS.

Antibodies. Anti-*Eh*PNT antibody was raised against purified *Eh*PNTdI in rabbit commercially (Operon, Tokyo, Japan). Anti-HA 11MO mouse monoclonal antibody was purchased from Berkeley Antibody (Berkeley, CA). Anti-*Eh*Sec61 α-subunit and anti-*E. histolytica* dolicol-*P*-mannose synthase (*Eh*DPMS) antibodies were a gift from Rosana Sánchez-López (37). Anti-galactose/*N*-acetylgalactosamine inhibitable lectin (Hgl) monoclonal antibody (3F4) (23) was a gift from Barbara J. Mann and William A. Petri, Jr. Alexa Fluor 488- or 568-conjugated anti-mouse and anti-rabbit IgGs were purchased from Invitrogen. Alkaline phosphatase-conjugated goat anti-rabbit and goat anti-mouse IgGs were bought from Jackson ImmunoResearch Laboratories (Bar Harbor, ME). Anti-GFP rabbit antibody was purchased from Medical Biological Laboratory International.

Immunoprecipitation. Approximately 3×10^6 cells of *Eh*PNT-HA- and Cpn60-HA-expressing amoebae were lysed in lysis buffer (50 mM Tris-HCl [pH 7.5], 150 mM NaCl, 1% Triton X-100, and 0.5 mg/ml E-64). The soluble lysate, after centrifugation at 15,000 × *g*, was incubated with protein G-Sepharose beads (30 μl of a 50% slurry) (Amersham Biosciences, Uppsala, Sweden) premixed with anti-HA antibody (0.5 μl) or anti-HA and anti-Hgl antibodies, respectively.

Immunoblot analysis. Whole-cell lysate and immunoprecipitated samples were separated on either a 12% or 15% (wt/vol) SDS-polyacrylamide gel and subsequently electrotransferred onto nitrocellulose membranes (Hybond-C Extra; Amersham Biosciences, Little Chalfont, Bucks, United Kingdom) as described previously (41). The membranes were blocked by incubation in 5% nonfat dried milk in TBST (50 mM Tris-HCl [pH 8.0], 150 mM NaCl, and 0.05% Tween 20) for 1.5 h at room temperature. The blots were reacted with primary anti-*Eh*PNT rabbit or anti-HA mouse antibody at a dilution of 1:500 to 1:1,000. The membranes were washed with TBST and further reacted with alkaline phosphatase-conjugated anti-rabbit or anti-mouse IgG antibody (1:1,000) at room temperature for 1.5 h. After further washing with TBST, specific proteins were visualized with an alkaline phosphatase conjugate substrate kit (Bio-Rad, Hercules, CA).

Deglycosylation of PNT. The *Eh*PNT-HA-expressing transformant was cultured with 3 μg/ml of tunicamycin (Sigma, St. Louis, MO) for 24 h to inhibit asparagine-linked glycosylation according to a protocol described previously (22). For the chemical deglycosylation of *Eh*PNT, *Eh*PNT and fetuin were dried in a Speed Vac. Ice-cold trifluoromethanesulfonic acid (TFMS)-anisol (3:2, vol/vol [100 μl]) was added, and the samples were incubated for 4 h at 4°C under N_2 according to a method described previously (13). The reaction was stopped by slowly adding 200 μl ice-cold H_2O-pyridine (73:10, vol/vol) containing 0.1% SDS to the mixture. Anisol was extracted three times with 250 μl ethyl ether. Dialysis was performed against 2 mM pyridine acetate buffer. After dialysis, the samples were subjected to SDS-PAGE and silver staining. Immunoprecipitated *Eh*PNT was also digested with PNGase F (New England Biolabs, Ipswich, MA), an amidase that cleaves between the innermost *N*-acetylglucosamine and asparagine residues of asparagine-linked glycoproteins, according to the manufacturer's instructions.

Immunofluorescence assay and organelle staining. Amoeba transformant or wild-type amoebae in a logarithmic growth phase were harvested, transferred into 8-mm round wells on glass slides, and incubated for 30 min at 35°C to let trophozoites attach to the glass surface. An indirect immunofluorescence assay was performed as previously described (36). Briefly, amoebae were fixed with 3.7% paraformaldehyde in PBS for 10 min at room temperature. The cells were then permeabilized with 0.05% Triton X-100 in PBS for 5 min. The samples were reacted with anti-*Eh*PNT (1:100), anti-*Eh*Sec61 α-subunit (1:30), anti-*Eh*DPMS antibody (1:30), anti-GFP (1:1,000) rabbit antibody, anti-HA (1:1,000) mouse antibody, or preimmune rabbit serum (1:100). The samples were then reacted with Alexa Fluor 488- or 568-conjugated anti-mouse or anti-rabbit IgG (1:1,000).

For the staining of endosomes or late endosomes/lysosomes, amoebae were incubated with BI-S-33 medium containing 2 mg/ml rhodamine isothiocyanate (RITC)-dextran for 10 to 60 min (for endosomes) or LysoTracker Red DND-99 (Molecular Probes, Eugene, OR) (1:500) for 12 h (for late endosomes/lysosomes), respectively. To visualize phagosomes, CHO cells prestained with 10 μM CellTracker Orange or 20 μM CellTracker Blue were added to *E. histolytica* trophozoites in 8-mm wells on a glass slide and incubated for 10 to 60 min. The samples were examined on an LSM 510 Meta confocal laser scanning microscope (Carl Zeiss, Thornwood, NY). Images were further analyzed by using LSM510 software.

RESULTS

Identification of two isotypes of PNT in *E. histolytica*. Two isozymes of PNT have been identified in the *E. histolytica* genome database at Pathema (http://pathema.tigr.org/tigr-scripts/pathema/) (EHI_055400 and EHI_014030, corresponding to GenBank accession numbers XP_001914099 and AAC41577, respectively). They showed 90% mutual amino acid identity. The latter *Eh*PNT isotype (EH_014030) is 1,083 aa long with a predicted molecular mass of 117.0 kDa and a pI of 5.39. This predicted protein is identical to the PNT protein previously reported (GenBank accession number AAC41577)

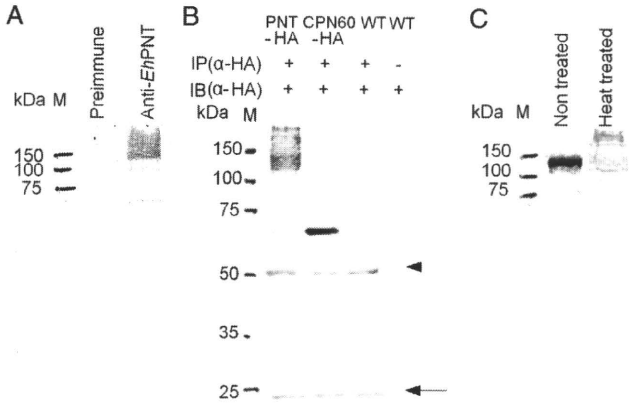

FIG. 1. Expression of PNT in *E. histolytica*. (A) Immunoblot analysis of native *Eh*PNT. Approximately 10 μg of total lysate was electrophoresed on a 12% SDS-polyacrylamide gel and subjected to an immunoblot assay with anti-*Eh*PNT antibody or preimmune serum. M, molecular mass marker. (B) Immunoprecipitation of *Eh*PNT. The lysates derived from the transformant expressing either *Eh*PNT-HA ("PNT-HA") or *Eh*Cpn60-HA ("CPN60-HA") and the wild-type strain ("WT") were subjected to immunoprecipitation with anti-HA antibody, followed by immunoblot analysis with anti-HA antibody. Lysate derived from the wild-type amoebae was also used directly for immunoblot analysis as a control. An arrowhead and an arrow indicate heavy and light chains of anti-HA antibody, respectively. IP, immunoprecipitation; IB, immunoblot. (C) Effect of heat treatment on the mobility of *Eh*PNT on an SDS-PAGE gel. Approximately 10 μg of total lysate was electrophoresed on a 12% SDS-polyacrylamide gel and subjected to an immunoblot assay with anti-*Eh*PNT antibody. M, molecular mass marker.

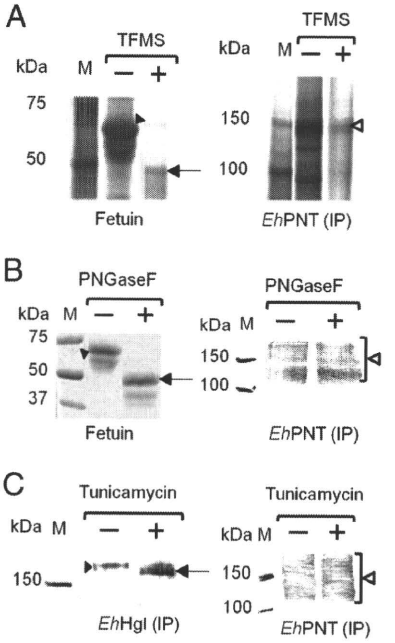

FIG. 2. Deglycosylation of *Eh*PNT. (A and B) Deglycosylation by TFMS or PNGase F. The lysates obtained from the transformant expressing *Eh*PNT-HA were subjected to immunoprecipitation (IP) with anti-HA antibody, followed by TFMS or PNGase F treatment and immunoblot detection with anti-HA antibody (right). Fetuin was used as a control, and gels were stained with silver (A) or Coomassie brilliant blue (B) (left). Filled arrowheads indicate untreated fetuin. Arrows indicate fetuin deglycosylated by TFMS (A) or PNGase F (B). Open arrowheads indicate *Eh*PNT. (C) Deglycosylation by tunicamycin. Lysates from the transformant expressing *Eh*PNT-HA cultured with tunicamycin were subjected to immunoprecipitation with either anti-*Eh*Hgl or anti-HA antibody, followed by immunoblot analysis with either anti-*Eh*Hgl or anti-HA antibody, respectively. A filled arrowhead or an arrow indicates untreated or deglycosylated *Eh*Hgl, respectively. An open arrowhead indicates *Eh*PNT.

(8). The dIII, dI, and dIIa regions of EHI_055400 (1,098 aa) are conserved except for a single amino acid substitution in dIII. EHI_055400 also contains a 5-aa extension at the amino terminus (MSLLL) and 9 aa substitutions in the putative TS (aa 1 to 14 of EHI_014030) (data not shown). In addition, dIIb of EHI_055400 contained 65 aa substitutions and two (4- and 6-aa-long) block insertions; the linker region also contains 24 aa substitutions. Since the domains involved in catalysis in EHI_055400 and EHI_014030 are totally conserved, and the two genes are expressed at comparable levels as steady-state mRNA by quantitative reverse transcriptase PCR (data not shown), we further studied only EHI_014030 in the present work. EHI_001930 (GenBank accession number XP_653216), which is annotated as the PNT β-subunit, showed no significant homology to either of the two *Eh*PNTs described above, while this sequence showed similarity with the β-subunit from other organisms and, thus, was excluded from this study.

Expression of PNT in *E. histolytica* trophozoites. Immunoblot analysis of the trophozoite lysate using anti-*Eh*PNT antibody showed a smear of >120 kDa (Fig. 1A). The size of the smear was unexpected because the predicted molecular masses of EHI_055400 and EHI_014030 were 119.0 and 117.0 kDa, respectively. To verify that this was not due to the cross-reactivity of anti-*Eh*PNT antibody, we immunoprecipitated *Eh*PNT from the *Eh*PNT-HA-expressing transformant with anti-HA antibody, followed by immunoblotting with anti-HA (Fig. 1B) or anti-*Eh*PNT (data not shown) antibody. Immunoprecipitated *Eh*PNT-HA was also recognized as a smear of >120 kDa, similar to that of endogenous *Eh*PNT.

To examine whether the smear was due to posttranslational modifications such as glycosylation, we treated immunoprecipitated *Eh*PNT-HA with TFMS or PNGase F. The pattern of immunoblots with anti-HA antibody was not affected, while the apparent molecular mass of control fetuin decreased (Fig. 2A and B). In addition, the treatment of the trophozoites with tunicamycin did not affect the mobility of *Eh*PNT, while the mobility of control Hgl increased (Fig. 2C). These data are consistent with the notion that *Eh*PNT is not glycosylated. We next examined whether aberrant mobility is due to unusual tertiary structures. We compared the patterns of the amoebic lysates, mixed with a one-third volume of 4× SDS-PAGE sample buffer (0.25 M Tris-HCl [pH 6.8], 8% SDS, and 8% 2-mercaptoethanol) and either incubated at 95°C for 5 min or left unheated, on SDS-PAGE gels. When the sample was electrophoresed without heating, *Eh*PNT was observed as a polypeptide of the predicted size (Fig. 1C). The exclusion of 2-mercaptoethanol did not affect mobility (data not shown). A similar observation was previously reported for membrane proteins, including serotonin transporter (24) and severe acute respiratory syndrome (SARS)-associated coronavirus mem-

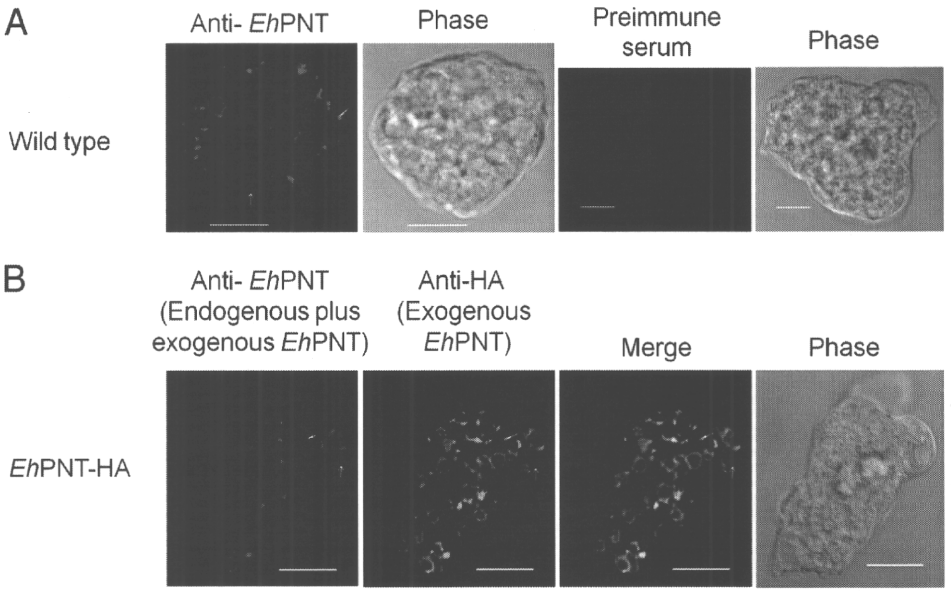

FIG. 3. (A) Subcellular localization of *Eh*PNT in wild-type amoebae. Wild-type amoebae were fixed, and an immunofluorescence assay was performed by using anti-*Eh*PNT (red) and preimmune sera. Bar, 10 μm. Arrows and arrowheads indicate representative vacuolar and dot-like structures of *Eh*PNT, respectively. (B) Colocalization of endogenous and exogenous epitope-tagged PNT in *E. histolytica*. *Eh*PNT-HA-overexpressing amoebae were fixed, and an immunofluorescence assay was performed by using anti-*Eh*PNT (red) and anti-HA (green) antibodies.

brane protein (18). In the latter case, three hydrophobic regions of 10 to 35 aa were shown to be responsible for the heat-induced aggregation of the membrane protein (18), suggesting that the heat-induced change of mobility of *Eh*PNT on SDS-PAGE is likely due to the hydrophobic nature of the protein.

Subcellular distribution of *Eh*PNT. An immunofluorescence assay using anti-*Eh*PNT antibody showed that *Eh*PNT is associated with the membranes of vesicles and vacuoles varying in size, or sometimes dot-like structures, scattered throughout the cytosol (Fig. 3A). We also examined the intracellular distribution of *Eh*PNT using the amoebic transformant that expressed *Eh*PNT (EHI_014030) with the carboxyl-terminal HA tag. The pattern of exogenous *Eh*PNT-HA (EHI_014030) and that of endogenous *Eh*PNT (a sum of EHI_055400 and EHI_014030) plus exogenous *Eh*PNT (EHI_014030) were indistinguishable (Fig. 3B). Since *Eh*PNT was previously postulated to be localized to mitosomes (8), we next examined the localization of *Eh*PNT and *Eh*Cpn60, the authentic marker of mitosomes, in the amoebic transformant expressing *Eh*Cpn60-HA (26) using anti-*Eh*PNT and anti-HA antibodies. No colocalization of *Eh*PNT and *Eh*Cpn60 was observed (Fig. 4).

Since *Eh*PNT was previously detected in isolated phagosomes (32, 33), we examined the localization of *Eh*PNT during the phagocytosis of CHO cells. Wild-type amoebae were incubated with CellTracker Orange-loaded CHO cells for 10 to 60 min to allow the ingestion of CHO cells. An immunofluorescence assay using anti-*Eh*PNT antibody (Fig. 5A) showed that the phagocytosed CHO cells were associated with *Eh*PNT at all time points (10, 20, and 60 min; only the images at 60 min are shown). The percentage of association gradually increased during the course of phagocytosis (65% ± 6%, 79% ± 9%, and 80% ± 8% at 10, 30, and 60 min, respectively). We then examined whether *Eh*PNT is localized to lysosomes using LysoTracker Red, a membrane-diffusible probe accumulated in acidic organelles (5). We found that the LysoTracker-labeled acidic compartment, the size and number of which were consistent with previous findings (28, 36), was associated with *Eh*PNT under steady-state conditions (79% ± 6% association) (Fig. 5B). To see whether *Eh*PNT is also associated with endosomes, we examined the localization of an endocytosed

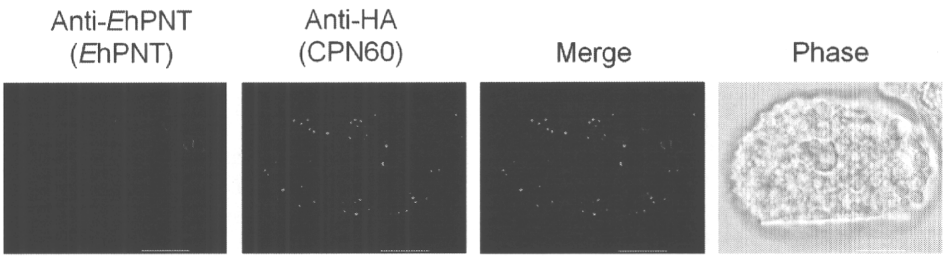

FIG. 4. Lack of association of *Eh*PNT with mitosomes. The amoebic transformant expressing *Eh*Cpn60-HA was stained with anti-HA (green) and anti-*Eh*PNT (red) antibodies to visualize *Eh*Cpn60 and *Eh*PNT, respectively. Bar, 10 μm.

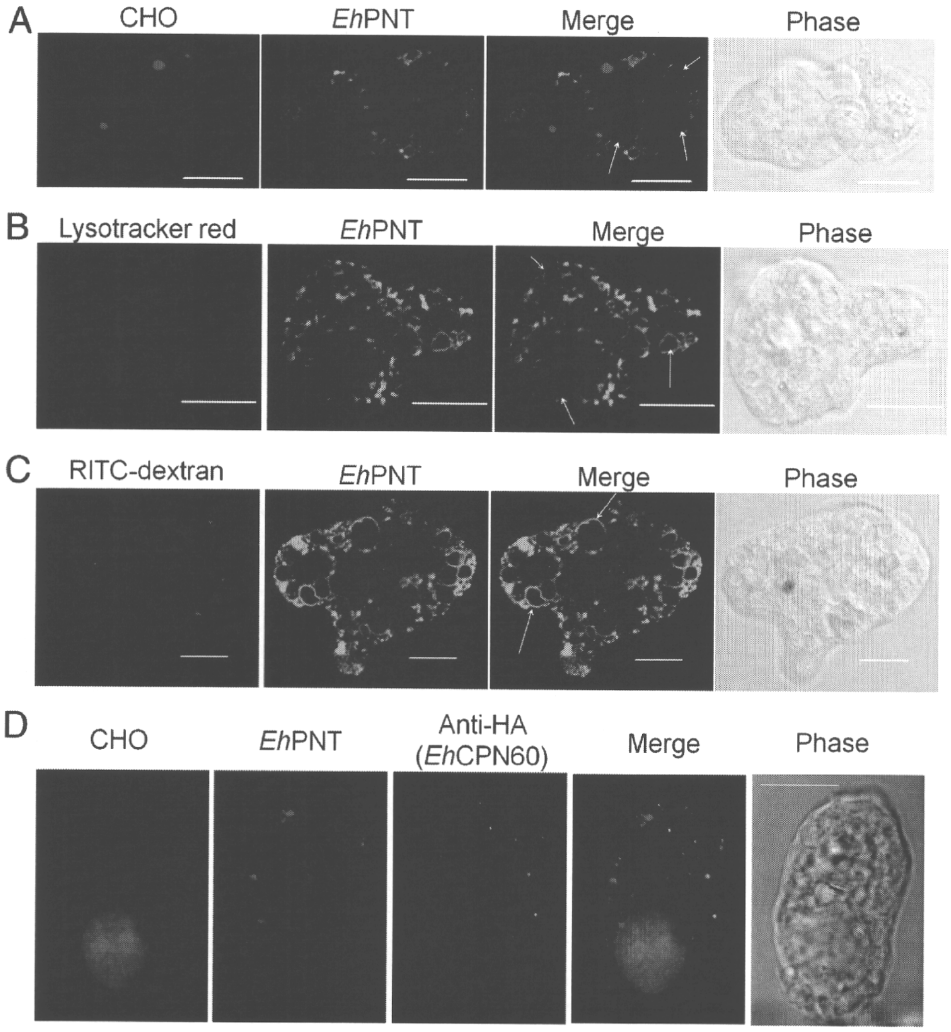

FIG. 5. Localization of *Eh*PNT to phagosomes, lysosomes, and endosomes. (A) Association of *Eh*PNT with phagosomes. Amoebae were incubated with CellTracker Orange-loaded CHO cells (red) for 60 min, fixed, and reacted with anti-*Eh*PNT antibody (green). Arrows indicate representative phagocytosed CHO cells associated with *Eh*PNT. (B) Association of *Eh*PNT with lysosomes. Amoebae were labeled with LysoTracker (red) and subjected to an immunofluorescence assay with anti-*Eh*PNT antibody (green). Arrows indicate representative lysosomes associated with *Eh*PNT. (C) Association of *Eh*PNT with the fluid-phase marker. Amoebae were incubated with medium containing RITC-dextran (red) for 1 h. The cells were fixed and reacted with anti-*Eh*PNT antibody (green). Arrows indicate representative endocytosed RITC-dextran associated with *Eh*PNT. (D) Subcellular localization of phagosomes, mitosomes, and *Eh*PNT. The amoebic transformant expressing *Eh*Cpn60-HA was incubated with CellTracker Blue-loaded CHO cells (blue) for 60 min, fixed, and reacted with anti-*Eh*PNT (red) and anti-*Eh*Cpn60 (green) antibodies. Bar, 10 μm.

fluid-phage marker, RITC-dextran. *Eh*PNT was only partially associated with RITC-dextran-containing endosomes, which were observed as tiny dot-like structures or a multivesicular body as previously shown (29), at each time point (10, 30, or 60 min; only the images at 60 min are shown) (Fig. 5C). We also examined whether *Eh*PNT is associated with mitosomes during the phagocytosis of CHO cells. An immunofluorescence assay using the amoebic transformant expressing *Eh*Cpn60-HA, CellTracker Blue-loaded CHO cells, anti-*Eh*PNT, and anti-HA antibody showed no colocalization of mitosomes and *Eh*PNT (Fig. 5D).

All domains are essential for the vesicular/vacuolar distribution of *Eh*PNT. To define the domain necessary for vesicular/vacuolar targeting of *Eh*PNT, we created amoeba transformants expressing the HA-tagged or GFP-fused protein containing various domains of PNT (Fig. 6A). The amoebic transformant expressing GFP fused with the 14-aa amino-terminal putative TS showed a cytoplasmic distribution (Fig. 6B), although the sequence MSTSSSIEEEVFNY appeared to contain the elements implicated for the TS (rich in hydroxylated and hydrophobic amino acids). The transformants expressing TS+dIIb-HA, TS+dIIb+dIII-HA, TS+dIIb+dIII+L-HA, or TS+dIIb+dIII+L+dI-HA showed a distribution that overlapped that of the endoplasmic reticulum (ER), visualized with anti-*Eh*Sec61 α-subunit antibody (27). The ER pattern was also confirmed with anti-*Eh*DPMS antibody (Fig. 6B). Full-length *Eh*PNT-HA did not overlap the ER visualized with either anti-*Eh*Sec61 α-subunit or anti-*Eh*DPMS antibody. Fractionation of the amoeba lysate followed by immunoblot analysis with anti-HA or anti-GFP an-

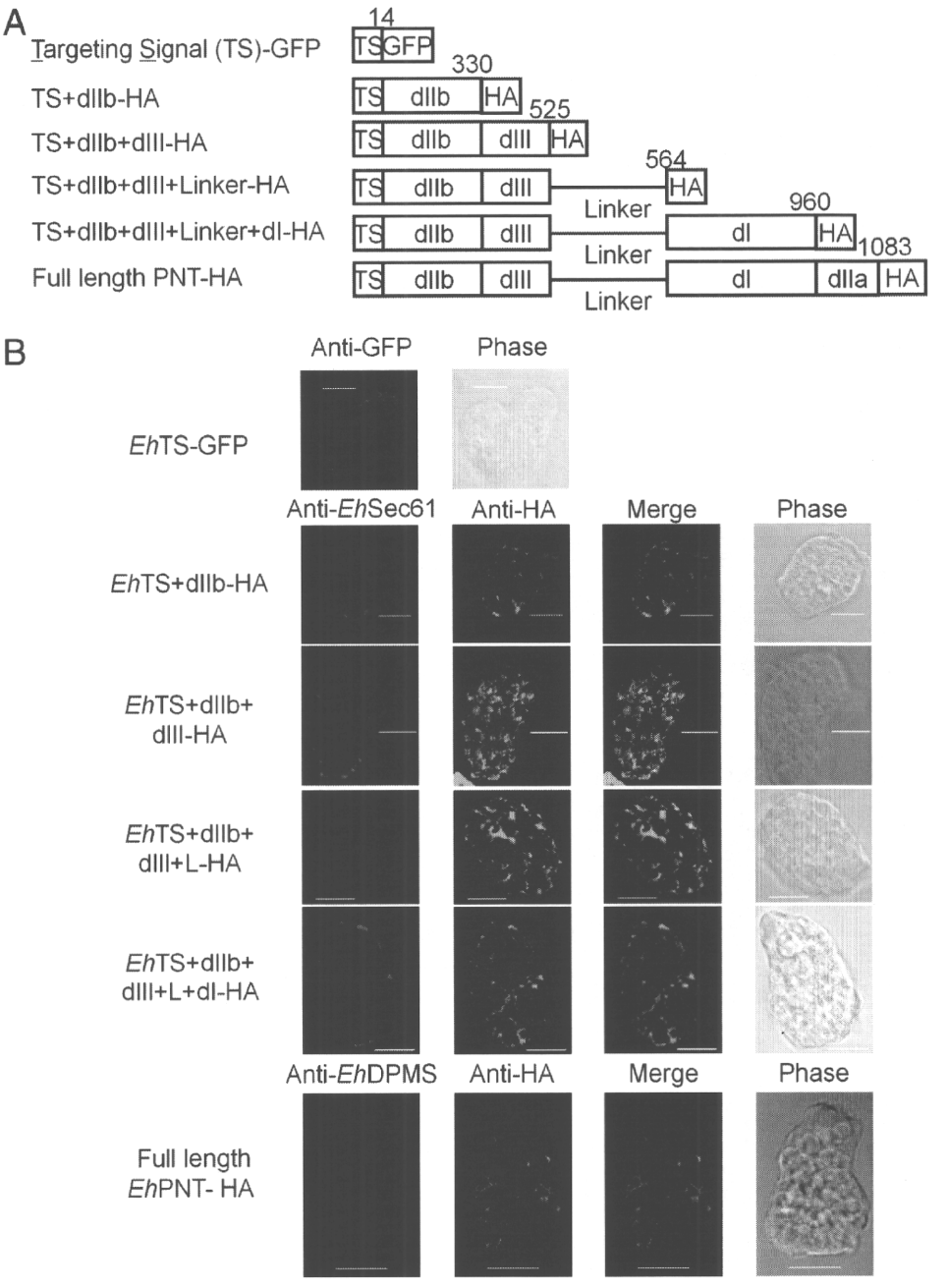

FIG. 6. Localization of a series of truncated *Eh*PNT proteins. (A) Schematic representation of HA epitope-tagged or GFP-fused recombinant *Eh*PNT used in the study. Domains, epitope (or GFP), and amino acid numbers are shown. (B) Localization of epitope-tagged or GFP-fused carboxyl-terminally truncated *Eh*PNT recombinant proteins. The transformants expressing *Eh*TS-GFP, *Eh*TS+dIIb-HA, *Eh*TS+dIIb+dIII-HA, *Eh*TS+dIIb+dIII+L-HA, and *Eh*TS+dIIb+dIII+L+dI-HA and *Eh*PNT-HA were subjected to an immunofluorescence assay using anti-HA (or anti-GFP for *Eh*TS-GFP) and anti-*Eh*Sec61 α-subunit (or anti-*Eh*DPMS for the *Eh*PNT-HA transformant) antibodies. Bar, 10 μm.

tibodies showed that all truncated forms of *Eh*PNT except for TS-GFP were partitioned into the 5,000 × *g* and 100,000 × *g* pellet fractions, while TS-GFP was fractionated into the 100,000 × *g* supernatant fraction (data not shown).

DISCUSSION

Mitosomes have been identified in several parasitic protozoan lineages such as *E. histolytica*, *Giardia intestinalis*, *Trachipleistophora hominis*, and *Cryptosporidium parvum* (21, 34, 42, 43, 50). *E. histolytica* was previously considered to be an early-branching "amitochondriate," as it lacks conventional mitochondria as well as other organelles typically found in most eukaryotes, such as peroxisomes, the rough ER, and the Golgi apparatus. However, the discovery of genes encoding the mitochondrial proteins Cpn60, PNT, mt-hsp70, ADP/ATP transporter, and Cpn10 (2, 7, 8, 21, 46) indicated that *E. histolytica* is the secondary "amito-

chondriate." While only a half-dozen proteins were shown to be localized to mitosomes (1, 2, 7, 8, 19, 21, 42, 44, 46), we recently discovered by proteomic analysis of isolated mitosomes that sulfate activation is the major pathway compartmentalized in mitosomes. Three enzymes consisting of the pathway and additional proteins required for the pathway, including sodium/sulfate symporter, mitochondrion carrier family protein, and chaperons, were identified in the mitosomal proteome. Although PNT was not discovered in the proteome, it was previously postulated to be mitosomal based on the resemblance of the amino-terminal region of *Eh*PNT to the potential mitochondrion-targeting peptide. However, it is important that the putative TS of *Eh*PNT is certainly not a canonical mitochondrion-targeting peptide because it lacks basic residues such as arginine or lysine.

Despite the premise, we showed, in this study, that *Eh*PNT was distributed to the membrane of vesicles and vacuoles, including lysosomes, phagosomes, and endosomes, but not to mitosomes. In addition, we showed that GFP fused with the amino-terminal putative TS of *Eh*PNT was distributed to the cytosol, which disproved the premise that the amino-terminal domain of *Eh*PNT functions as a putative organelle-targeting sequence. The 15-aa-long amino terminus of Cpn60 was not sufficient for the targeting of either luciferase or GFP to mitosomes (1; our unpublished data), although the removal of the first 15 aa of Cpn60 caused a mislocalization of the protein in the cytoplasm (42). Therefore, a role of the amino-terminal transit peptide for mitosomal transport remains obscure.

The association of PNT with the acidified compartments (lysosomes and phagosomes) (Fig. 5) is unprecedented in eukaryotes, where PNT is usually localized to the inner membrane of mitochondria (48). The dependence of transhydrogenase activity of *Eh*PNT on pH was demonstrated; the rate of transhydrogenation was higher at an acidic pH (5.5) than at a neutral pH (7.0 to 8.0) (49). The generation of NADPH by membrane-associated PNT (49) depends upon a proton-motive force, which is likely generated by V-ATPase localized to the acidified compartment and also the nonacidified compartment. While the colocalization of V-ATPase and *Eh*PNT has not been directly demonstrated, phagosomes contained major components of V-ATPase, as shown by the proteomic analysis of purified phagosomes (32, 33). Therefore, it is conceivable that amebic PNT localized in the acidic environment possesses enzymological properties suitable for acidic environments. Since our attempt to repress *Eh*PNT expression by gene silencing failed (our unpublished data), the physiological role of *Eh*PNT has not been elucidated. However, *Eh*PNT may be involved in the detoxification of reactive oxygen and nitrogen species by supplying NADPH as a reducing power by using a proton gradient across the lysosomal and phagosomal membranes. During tissue invasion, *E. histolytica* adapts to changing oxygen tensions as it goes from the anaerobic colonic lumen to an oxygen-rich environment in the tissue (40). Additionally, the parasite must cope with cytotoxic reactive oxygen and nitrogen species that are produced and released by activated phagocytes that are attracted to the site of infection (4, 20, 40).

Although we cannot exclude the possibility that truncated *Eh*PNT was misfolded and aggregated in the cell, our immunofluorescence and cellular fractionation data are consistent with the premise that all truncated *Eh*PNT was retained in the ER, which is suggestive of the default mechanisms of retention of multiple transmembrane proteins in the ER. The possibility that truncated *Eh*PNT is retained in the heavy microsomal fraction was previously suggested (1), where the majority (93%) of luciferase activity of the recombinant protein consisted of the 67-aa-long amino-terminal portion of PNT fused to firefly luciferase was associated with the mixed membrane fraction and was as susceptible to trypsin degradation as cytosolic luciferase from control parasites. Our present data also support the interpretation of the study that the fusion protein is embedded in the ER membrane and not targeted to mitosomes. We also showed that the aberrant mobility of PNT on SDS-PAGE gels (Fig. 1) was not likely due to either N-linked or O-linked glycosylation but was due to the hydrophobic nature of *Eh*PNT. Altogether, *E. histolytica* PNT represents a novel class of PNT localized to lysosomes and appears to have evolved uniquely in this organism.

ACKNOWLEDGMENTS

We thank Rosana Sánchez-López, Universidad Nacional Autónoma de México, for anti-*Eh*Sec61 α-subunit and anti-*Eh*DPMS antibodies and Barbara J. Mann and William A. Petri, Jr., University of Virginia Health System, for anti-Hgl antibody (3F4). We also thank Takashi Makiuchi for helpful discussions.

This work was supported by a grant-in-aid for creative scientific research (grant 18GS0314) and a grant-in-aid for scientific research (grants 18GS0314, 18050006, and 18073001) from the Ministry of Education, Culture, Sports, Science, and Technology of Japan to T.N.; a grant for Research on Emerging and Re-Emerging Infectious Diseases from the Ministry of Health, Labor, and Welfare of Japan (grant H20-Shinkosaiko-Ippan-016); and a grant for research to promote the development of anti-AIDS pharmaceuticals from the Japan Health Sciences Foundation to T.N. (grant KAA1551).

REFERENCES

1. **Aguilera, P., T. Barry, and J. Tovar.** 2008. *Entamoeba histolytica* mitosomes: organelles in search of a function. Exp. Parasitol. **118:**10–16.
2. **Bakatselou, C., C. Kidgell, and C. C. Clark.** 2000. A mitochondrial-type hsp70 gene of *Entamoeba histolytica*. Mol. Biochem. Parasitol. **110:**177–182.
3. **Bizouarn, T., O. Fjellstrom, J. Meuller, M. Axelsson, A. Bergkvist, C. Johansson, G. Karlsson, and J. Rydstrom.** 2000. Proton translocating nicotinamide nucleotide transhydrogenase from *E. coli*. Mechanism of action deduced from its structural and catalytic properties. Biochim. Biophys. Acta **1457:**211–228.
4. **Bogdan, C., M. Rollinghoff, and A. Diefenbach.** 2000. Reactive oxygen and reactive nitrogen intermediates in innate and specific immunity. Curr. Opin. Immunol. **12:**64–76.
5. **Bucci, C., P. Thomsen, P. Nicoziani, J. McCarthy, and B. van Deurs.** 2000. Rab7: a key to lysosome biogenesis. Mol. Biol. Cell **11:**467–480.
6. **Carlton, J. M., S. V. Angiuoli, and D. J. Carucci.** 2002. Genome sequence and comparative analysis of the model rodent malaria parasite *Plasmodium yoelii*. Nature **419:**512–519.
7. **Chan, K. W., D. J. Slotboom, S. Cox, T. M. Embley, O. Fabre, M. van der Giezen, M. Harding, D. S. Horner, E. R. Kunji, G. Leon-Avila, and J. Tovar.** 2005. A novel ADP/ATP transporter in the mitosome of the microaerophilic human parasite *Entamoeba histolytica*. Curr. Biol. **15:**737–742.
8. **Clark, C. G., and A. J. Roger.** 1995. Direct evidence for secondary loss of mitochondria in *Entamoeba histolytica*. Proc. Natl. Acad. Sci. U. S. A. **92:** 6518–6521.
9. **Diamond, L. S., D. R. Harlow, and C. C. Cunnick.** 1978. A new medium for the axenic cultivation of *Entamoeba histolytica* and other *Entamoeba*. Trans. R. Soc. Trop. Med. Hyg. **72:**431–432.
10. **Gardner, M. J., and B. Barrell.** 2002. Genome sequence of the human malaria parasite *Plasmodium falciparum*. Nature **419:**498–511.
11. **Gill, E. E., S. Diaz-Triviño, M. J. Barberà, J. D. Silberman, A. Stechmann, D. Gaston, I. Tamas, and A. J. Roger.** 2007. Novel mitochondrion-related organelles in the anaerobic amoeba *Mastigamoeba balamuthi*. Mol. Microbiol. **66:**1306–1320.
12. **Hall, N., M. Karras, and R. E. Sinden.** 2005. A comprehensive survey of the *Plasmodium* life cycle by genomic, transcriptomic, and proteomic analyses. Science **307:**82–86.
13. **Hiltpold, A., M. Frey, A. Hulsmeier, and P. Kohler.** 2000. Glycosylation and

palmitoylation are common modifications of *Giardia* variant surface proteins. Mol. Biochem. Parasitol. **109:**61–65.
14. **Hoek, J. B., and J. Rydstrom.** 1988. Physiological roles of nicotinamide nucleotide transhydrogenase. Biochem. J. **254:**1–10.
15. **Jackson, J. B.** 1991. The proton-translocating nicotinamide adenine dinucleotide transhydrogenase. J. Bioenerg. Biomembr. **23:**715–741.
16. **Jackson, J. B., S. J. Peake, and S. A. White.** 1999. Structure and mechanism of proton-translocating transhydrogenase. FEBS Lett. **464:**1–8.
17. **Kramer, R. A., L. A. Tomchak, S. J. McAndrew, K. Becker, D. Hug, L. Pasamontes, and M. Humbelin.** 1993. An *Eimeria tenella* gene encoding a protein with homology to the nucleotide transhydrogenases of *Escherichia coli* and bovine mitochondria. Mol. Biochem. Parasitol. **60:**327–331.
18. **Lee, Y.-N., L.-K. Chen, H.-C. Ma, H.-H. Yang, H.-P. Li, and S.-Y. Lo.** 2005. Thermal aggregation of SARS-CoV membrane protein. J. Virol. Methods **129:**152–161.
19. **Leon-Avila, G., and J. Tovar.** 2004. Mitosomes of *Entamoeba histolytica* are abundant mitochondrion-related remnant organelles that lack a detectable organeller genome. Microbiology **150:**1245–1250.
20. **MacMicking, J., Q. W. Xie, and C. Nathan.** 1997. Nitric oxide and macrophage function. Annu. Rev. Immunol. **15:**323–350.
21. **Mai, Z., S. Ghosh, M. Frisardi, B. Rosenthal, R. Rogers, and J. Samuelson.** 1999. Hsp60 is targeted to a cryptic mitochondrion-derived organelle ("crypton") in the microaerophilic protozoan parasite *Entamoeba histolytica*. Mol. Cell. Biol. **19:**2198–2205.
22. **Mann, B. J., B. E. Torian, T. S. Vedvick, and W. A. Petri, Jr.** 1991. Sequence of a cysteine-rich galactose-specific lectin of *Entamoeba histolytica*. Proc. Natl. Acad. Sci. U. S. A. **88:**3248–3252.
23. **Mann, B. J., C. Y. Chung, J. M. Dodson, L. S. Ashley, L. L. Braga, and T. L. Snodgrass.** 1993. Neutralizing monoclonal antibody epitopes of the *Entamoeba histolytica* galactose adhesin map to the cysteine-rich extracellular domain of the 170-kilodalton subunit. Infect. Immun. **61:**1772–1778.
23a. **Maralikova, B., V. Ali, K. Nakada-Tsukui, T. Nozaki, M. van der Giezen, K. Henze, and J. Tovar.** 2010. Bacterial-type oxygen detoxification and iron-sulfur cluster assembly in amoebal relict mitochondria. Cell. Microbiol. **12:** 331–342.
24. **McLane, M. W., G. Hatzidimitriou, J. Yuan, U. McCann, and G. Ricaurte.** 2007. Heating induces aggregation and decreases detection of serotonin transporter protein on Western blots. Synapse **61:**875–876.
25. **Meza, I.** 1992. *Entamoeba histolytica*: phylogenetic consideration. Arch. Med. Res. **23:**1–5.
26. **Mi-ichi, F., M. A. Yousuf, K. Nakada-Tsukui, and T. Nozaki.** 2009. Mitosomes in *Entamoeba histolytica* contain a sulphate activation pathway. Proc. Natl. Acad. Sci. U. S. A. **106:**21731–21736.
27. **Mitra, B. N., Y. Saito-Nakano, K. Nakada-Tsukui, D. Sato, and T. Nozaki.** 2007. Rab11B small GTPase regulates secretion of cysteine proteases in the enteric protozoan parasite *Entamoeba histolytica*. Cell. Microbiol. **9:**2112–2125.
28. **Nakada-Tsukui, K., Y. Saito-Nakano, V. Ali, and T. Nozaki.** 2005. A retromerlike complex is a novel Rab7 effector that is involved in the transport of the virulence factor cysteine protease in the enteric protozoan parasite *Entamoeba histolytica*. Mol. Biol. Cell **16:**5294–5303.
29. **Nakada-Tsukui, K., H. Okada, B. N. Mitra, and T. Nozaki.** 2009. Phosphatidylinositol-phosphates mediate cytoskeletal reorganization during phagocytosis via a unique modular protein consisting of RhoGEF/DH and FYVE domains in the parasitic protozoon *Entamoeba histolytica*. Cell. Microbiol. **11:**1471–1491.
30. **Nozaki, T., T. Asai, L. B. Sanchez, S. Kobayashi, and M. Nakazawa.** 1999. Characterization of the gene encoding serine acetyltransferase, a regulated enzyme of cysteine biosynthesis from the protist parasites *Entamoeba histolytica* and *Entamoeba dispar*. Regulation and possible function of the cysteine biosynthetic pathway in *Entamoeba*. J. Biol. Chem. **274:**32445–32452.
31. **Nozaki, T., T. Asai, S. Kobayashi, F. Ikegami, M. Noji, K. Saito, and T. Takeuchi.** 1998. Molecular cloning and characterization of the genes encoding two isoforms of cysteine synthase in the enteric protozoan parasite *Entamoeba histolytica*. Mol. Biochem. Parasitol. **97:**33–44.
32. **Okada, M., C. D. Huston, B. J. Mann, W. A. Petri, Jr., K. Kita, and T. Nozaki.** 2005. Proteomic analysis of phagocytosis in the enteric protozoan parasite *Entamoeba histolytica*. Eukaryot. Cell **4:**827–831.
33. **Okada, M., C. D. Huston, M. Oue, B. J. Mann, W. A. Petri, Jr., K. Kita, and T. Nozaki.** 2006. Kinetics and strain variation of phagosome proteins of *Entamoeba histolytica* by proteomic analysis. Mol. Biochem. Parasitol. **145:** 171–183.
34. **Riordan, C. E., J. G. Ault, S. G. Langreth, and J. S. Keithly.** 2003. *Cryptosporidium parvum* Cpn60 targets a relict organelle. Curr. Genet. **44:**138–147.
35. **Roger, A. J., S. G. Svard, J. Tovar, C. G. Clark, M. W. Smith, F. D. Gillin, and M. L. Sogin.** 1998. A mitochondrial-like chaperonin 60 gene in *Giardia lamblia*: evidence that diplomonads once harboured an endosymbiont related to the progenitor of mitochondria. Proc. Natl. Acad. Sci. U. S. A. **95:**229–234.
36. **Saito-Nakano, Y., T. Yasuda, K. Nakada-Tsukui, M. Leippe, and T. Nozaki.** 2004. Rab5-associated vacuoles play a unique role in phagocytosis of the enteric protozoan parasite *Entamoeba histolytica*. J. Biol. Chem. **279:**49497–49507.
37. **Salgado, M., J. C. Villagómez-Castro, R. Rocha-Rodríguez, M. Sabanero-López, M. A. Ramos, A. Alagón, E. López-Romero, and R. Sánchez-López.** 2005. *Entamoeba histolytica*: biochemical and molecular insights into the activities within microsomal fractions. Exp. Parasitol. **110:**363–373.
38. **Sambrook, J., and D. W. Russell.** 2001. Molecular cloning: a laboratory manual, 3rd ed. Cold Spring Harbor Laboratory Press, Cold Spring Harbor, NY.
39. **Sazanov, L. A., and J. B. Jackson.** 1994. Proton-translocating transhydrogenase and NAD- and NADP-linked isocitrate dehydrogenases operate in a substrate cycle which contributes to fine regulation of the tricarboxylic acid cycle activity in mitochondria. FEBS Lett. **344:**109–116.
40. **Stanley, S. L., Jr.** 2003. Amoebiasis. Lancet **361:**1025–1034.
41. **Tokoro, M., T. Asai, S. Kobayashi, T. Takeuchi, and T. Nozaki.** 2003. Identification and characterization of two isoenzymes of methionine γ-lyase from *Entamoeba histolytica*: a key enzyme of sulfur-amino acid degradation in an anaerobic parasitic protist that lacks forward and reverse trans-sulfuration pathways. J. Biol. Chem. **278:**42717–42727.
42. **Tovar, J., A. Fischer, and C. G. Clark.** 1999. The mitosome, a novel organelle related to mitochondria in the amitochondrial parasite *Entamoeba histolytica*. Mol. Microbiol. **32:**1013–1021.
43. **Tovar, J., G. Leon-Avila, L. B. Sanchez, R. Sutak, J. Tachezy, and M. van der Giezen.** 2003. Mitochondrial remnant organelles of *Giardia* function in iron-sulphur protein maturation. Nature **426:**172–176.
44. **Tovar, J., S. S. E. Cox, and M. van der Giezen.** 2007. A mitosome purification protocol based on Percoll density gradients and its use in validating the mitosomal nature of *Entamoeba histolytica* mitochondrial Hsp70. Methods Mol. Biol. **390:**167–177.
45. **van der Giezen, M.** 2009. Hydrogenosomes and mitosomes: conservation and evolution of functions. J. Eukaryot. Microbiol. **56:**221–231.
46. **van der Giezen, M., G. Leon-Avila, and J. Tovar.** 2005. Characterization of chaperonin 10 (Cpn10) from the intestinal human pathogen *Entamoeba histolytica*. Microbiology **151:**3107–3115.
47. **Vermeulen, A. N., J. J. Kok, P. Van Den Boogart, R. Dijkema, and J. A. J. Claessens.** 1993. *Eimeria* refractile body proteins contain two potentially functional characteristics: transhydrogenase and carbohydrate transport. FEMS Microbiol. Lett. **110:**223–229.
48. **Weston, C. J., J. D. Venning, and J. B. Jackson.** 2002. The membrane-peripheral subunits of transhydrogenase from *Entamoeba histolytica* are functional only when dimerized. J. Biol. Chem. **277:**26163–26170.
49. **Weston, C. J., S. A. White, and J. B. Jackson.** 2001. The unusual transhydrogenase of *Entamoeba histolytica*. FEBS Lett. **488:**51–54.
50. **Williams, B. A., R. P. Hirt, J. M. Lucocq, and T. M. Embley.** 2002. A mitochondrial remnant in the microsporidian *Trachipleistophora hominis*. Nature **418:**865–869.
51. **Yu, Y., and J. Samuelson.** 1994. Primary structure of an *Entamoeba histolytica* nicotinamide nucleotide transhydrogenase. Mol. Biochem. Parasitol. **68:**323–328.

Tropical Medicine and Health Vol. 39 No. 1, 2011, pp. 1-14

Review

The Global Programme to Eliminate Lymphatic Filariasis: History and achievements with special reference to annual single-dose treatment with diethylcarbamazine in Samoa and Fiji

Eisaku Kimura

Abstract: Diethylcarbamazine (DEC), first introduced in 1947, was shown to have strong efficacy and safety for treatment of human lymphatic filariasis, which is caused mostly by a species *Wuchereria bancrofti*. Many studies to optimize the dosage and treatment schedule of DEC followed, and, based on the results, control programs with various regimens were implemented in different endemic areas/countries. By the mid 1970s, with endorsement by the WHO Expert Committee on Filariasis (3rd report, 1974), the standard DEC regimen for *W. bancrofti* infection in mass treatment had been established in principle: a total dose of 72 mg/kg of body weight given in 12 divided doses, once weekly or monthly, at 6 mg/kg each. Not long after the committee report, the efficacy of annual single-dose treatment at 6 mg/kg, which is only one twelfth of the WHO-recommended dose in a year, was reported effective in French Polynesia (study period: 1973-78), and later in Samoa (study period: 1979-81). These results were published between 1978 and 1985 in the Bulletin of WHO but received little attention. In the mid 1980s, the efficacy of ivermectin, the first-choice drug for onchocerciasis, against lymphatic filariae came to light. Since the effect at a single dose was remarkable, and often better than DEC, it was predicted that the newly introduced drug would replace DEC. Treatment experiments with ivermectin increased quickly in number. Meanwhile, annual single-dose mass drug administration (MDA) with DEC at 6 mg/kg was under scrutiny in Samoa and Fiji. In the early 1990s, the Samoan study, which covered the entire population of 160,000 with 3 annual MDAs, reported a significant reduction in microfilaria (mf) prevalence and mean mf density, while in Fiji, the efficacy of 5 rounds of annual MDA (total dose, 30 mg/kg) was shown to be as effective as 28 multi-dose MDA spread over 2 years (6 weekly plus 22 monthly treatments at 5 mg/kg; total dose, 140 mg/kg). Several additional studies carried out in Samoa in relation to the annual single-dose MDAs revealed that low density mf carriers, who have a very low mf count of 1-20/ml of venous blood, could not play a significant role in filariasis transmission.

From around 1990, studies on spaced low-dose DEC treatments and various types of combination chemotherapy with DEC and ivermectin increased. Albendazole, a well-known anti-intestinal helminths agent, was later added to the combination. The main findings of these studies with *W. bancrofti* are: (i) a single dose of DEC at 6 mg/kg reduced mean mf density by ca. 90% 1 year after treatment; (ii) the same dose could damage/kill adult worms; (iii) a single dose of ivermectin at ca. 400 μg/kg was more effective than DEC in reducing mf density during the first year and was similarly or less effective in the second year; (iv) ivermectin probably could not kill adult worms; (v) a single combined dose of albendazole (400 mg) and DEC (6 mg/kg) was effective to reduce mf density by 85 to nearly 100% 12-24 months after treatment; and (vi) ivermectin or albendazole included in the combination chemotherapy produced "beyond-filariasis" benefits: clearance/reduction of intestinal helminths, and, additionally, in the case of ivermectin, skin-dwelling ectoparasites.

The Global Programme to Eliminate Lymphatic Filariasis (GPELF) started its worldwide activities in 2000, with the target of elimination by 2020. The basic strategy is to conduct annual single-dose MDAs for 4-6 years. In 2000-2007, a minimum of 570 million individuals were treated in 48 of 83 endemic countries. The drugs used are DEC 6 mg/kg plus albendazole 400 mg in most countries, or ivermectin 200-400 μg/kg plus albendazole 400 mg particularly in onchocerciasis endemic countries in Africa. (MDAs with DEC alone had been used in India.)

The GPELF achieved impressive results in terms of parasitological cure/improvement, clinical benefits, social and economic impacts, etc. However, the most impressive result of all was the programme's success in mobilizing hundreds of millions of local people, who not only took drugs but many of them actively supported MDAs as drug distributors and volunteers. Beyond filariasis, the role people can play in supplementing rural health services is now a topic of discussion and a source of hope for a new sustainable system.

Keywords: Lymphatic filariasis, global programme for elimination, diethylcarbamazine, albendazole, ivermectin, annual single-dose, mass drug administration, Samoa, Fiji

Department of Parasitology, Aichi Medical University, 21 Karimata, Yazako, Aichi-gun, Aichi-ken, Japan
Tel: 0561-62-3311
Fax: 0561-63-3645
Email: kimura@aichi-med-u.ac.jp

A. Introduction

a-1. *Parasite and disease*

Human lymphatic filariae, which are characterized by the parasitism of their adult worms in the lymphatic system, include 3 species, *Wuchereria bancrofti*, *Brugia malayi* and *Brugia timori*. Female adults reproduce offspring or microfilariae (mf) which are carried into blood circulation by the lymph flow and accumulate in the lungs. Mf are released from the lungs into the circulation at night (nocturnal periodicity of mf), synchronizing with the circadian biting cycle of mosquitoes that transmit the parasite between humans. In some Pacific islands, where *Aedes* mosquitoes bite humans in the daytime, the release from the lungs is mainly in the afternoon (diurnally subperiodicity). The detection of mf in blood is a basic method of diagnosis. After being ingested by mosquito vectors, mf develop to the infective stage of larvae in about 10-14 days. When mosquitoes with infective larvae bite humans, filarial parasites have an opportunity to enter the host. Infective larvae, males and females, penetrate the human skin, migrate in the body and reach the lymphatic system where they mature, mate and reproduce mf in about 6-12 months after skin invasion. Adult worms will damage and dilate lymphatic vessels, and cause lymphostasis often in the lower limb and around the testes and kidney. This is the basic pathology of chronic filariasis characterized by lymphedema, hydrocele, and chyluria. Lymphedema often triggers secondary bacterial infections resulting in acute fever attacks (acute dermatolymphangioadenitis [1]), which aggravate lymphedema/inflammation. In some people, the edematous skin gradually thickens, hardens and may grow to wart-like lesions. The word 'elephantiasis' refers to this condition with the often serious deformities that have caused enormous suffering among affected people worldwide for thousands of years (Fig. 1) [2].

a-2. *Epidemiology and global efforts to eliminate lymphatic filariasis*

The total number of lymphatic filariasis cases in the world, as estimated in 1996 [3], was 120 million, about 90% of which were caused by *W. bancrofti*. The total figure includes 16 million lymphedema (including elephantiasis) and 27 million hydrocele cases, the rest being cases with microfilaremia only. The infection was more prevalent among males, and adults. By region/country, India and sub-Saharan Africa had more than 40 million cases each, followed by other Asia and Islands (ca. 20 mil.) and China (ca. 10 mil.). With the swollen leg and/or scrotum, lymphatic filariasis was ranked as the 4th leading cause of permanent and long-term disability [4]. Most of the patients have been neglected and suffer from mental distress, social isolation, and economic misery due to the stigma of the disfiguring disease [5]. The estimated disability-adjusted life years (DALYs) lost in 1999 was 4.92 million [6]. As for economic loss, in India alone, the cost of treatment for acute fever attacks and chronic symptoms reached an estimated US$ 31.1 million per year, and the loss of productivity US$ 811 million per year [7].

These gloomy statistics have changed rapidly for the better since the Global Programme to Eliminate Lymphatic Filariasis (GPELF) started in 2000 (details in Section F). The Global Alliance to Eliminate Lymphatic Filariasis (GAELF) was formed the same year to support the unprecedented global program. The alliance includes health ministries of endemic countries, UN agencies (especially WHO as the secretariat), the private sector, NGDOs, academia, and government bodies (including JICA). Particularly noteworthy are the contributions of two pharmaceutical companies: GlaxoSmithKline donates albendazole free of charge and Merck & C., Inc. ivermectin. Both drugs are essential for the Mass Drug Administration (MDA) carried out annually in endemic countries. In 2007, 48 out of 81 endemic countries conducted MDAs, and 546 million people in the world were treated for lymphatic filariasis. The same year, China declared the elimination of filariasis, which was followed by Korea's declaration in 2008 [8].

B. The "new" anti-filarial drug diethylcarbamazine (DEC): Early studies to find the optimal dosage

b-1. *Trials with multi-dose treatment*

The anti-filarial effect of 1-diethylcarbamyl-4-methylpiperazine hydrochloride (DEC hydrochloride) was first reported in 1947 by Hewitt et al. [9] using naturally acquired filarial parasites in cotton rats (*Litomosoides carinii*) and dogs (*Dirofilaria immitis*). The same drug was tried for human bancroftian filariasis and its microfilaricidal and possible adulticidal effects were confirmed the following year [10]. A series of experimental treatments was conducted using DEC citrate for DEC hydrochloride to determine suitable dosage and treatment schedule. Many important studies were carried out in the South Pacific islands, where more than 10,000 American soldiers suffered clinical filariasis due to diurnally subperiodic *W. bancrofti* during World War II [11].

In American Samoa, 5 different multi-dose trials with DEC (3-9 mg/kg of body weight per day for 7-30 days, total dosage 21-270 mg/kg) confirmed rapid microfilaricidal effects, but the treatments could not prevent the reappearance of mf in 2-year follow-up studies (reported in 1953 [12]). Using 111-175 mf positives, Mahoney & Kessel [13] reported in 1971 that DEC given at 6 mg/kg daily for 6 days

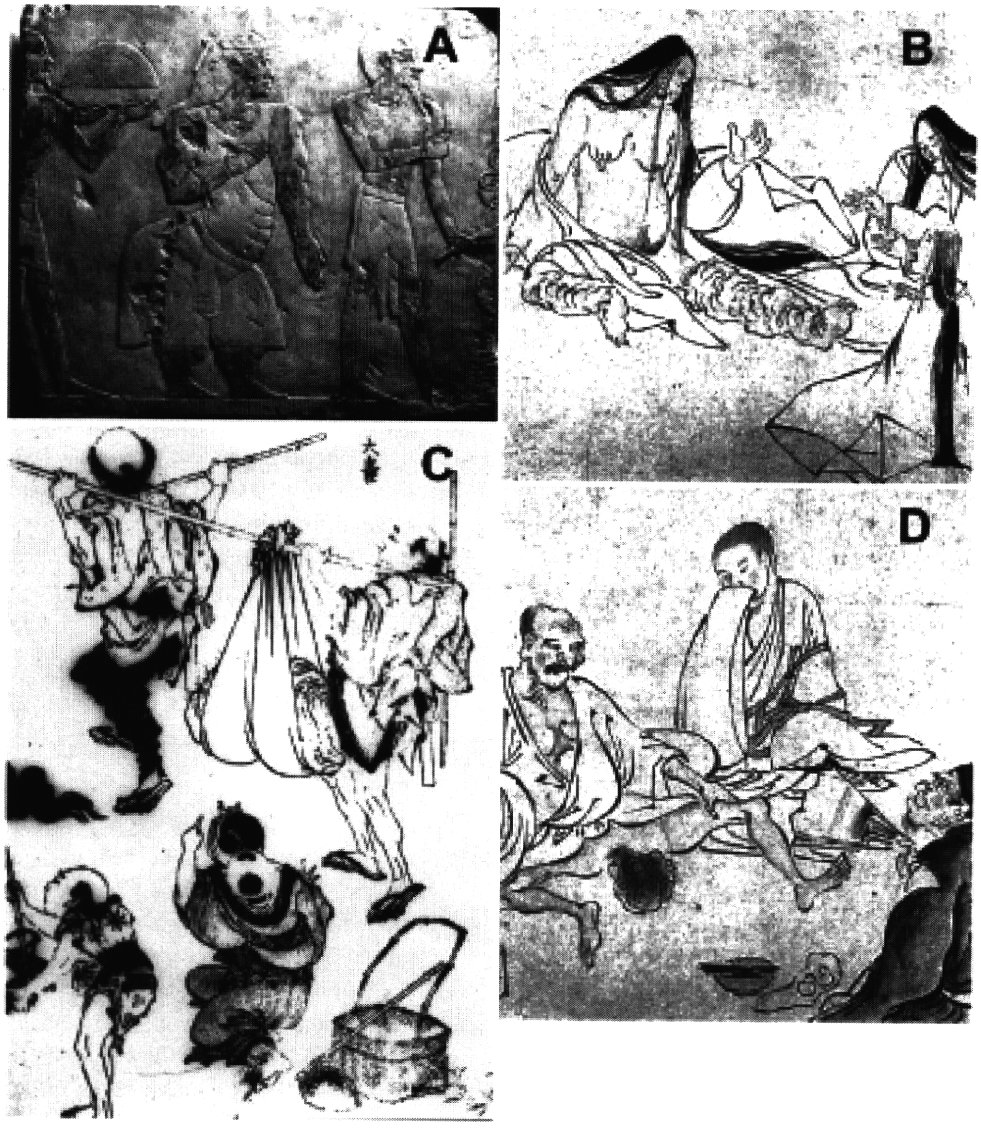

Fig. 1 Chronic symptoms of lymphatic filariasis
A: An Egyptian relief from Queen Hatshepsut's temple, Luxor, depicting the Princess of Punt, a possible elephantiasis case. (The Queen's reign: 1503-1482 B.C.); B and D: Elephantiasis of the legs and scrotum, described some 1,000 years ago in "Strange Diseases Picture Scroll." (Kyoto National Museum, Japan); C: Huge elephantiasis of the scrotum, painted by Hokusai Katsushika (1760-1849). Manga in the Edo era of Japan. {From Ref. [2], courtesy of Prof. Yoshihito Otsuji}

resulted in 32% persistence (rate of mf positive 1 week after treatment) and that the recurrence rate was 24% (rate of mf reappearance within 1 year of treatment). In this study, the diagnosis of infection was made by the detection of mf in 20 μl capillary blood obtained by the finger-prick (F-P) method.

In Fiji, Manson-Bahr (1952) [14] conducted treatment experiments with Hetrazan (DEC) at 100-300 mg daily for 15 to over 70 days and concluded that treatment must be continuous for at least two months. This conclusion was based on a finding that, even after multi-dose treatments cleared mf in 20 μl of F-P blood, mf were still positive when 1 ml of venous blood was examined by Knott's method. Burnet & Mataika (1961) [15] administered 6 weekly doses of DEC at 400 mg (ca. 5-8 mg/kg) each and repeated the same regimen half a year later (total dosage 4,800 mg). The treatment reduced mf rate, determined with 60 μl of F-P blood, from 12.2% to 2.7%. However, they noted that over 40% of mf negatives (who had been positive before treatment) were in fact positive by Knott's method

using 1 ml of venous blood.

In French Polynesia, Kessel (1957) [16] compared 3 different dosages and reported that 6 mg/kg once a month for 24 months showed the best result in terms of mf prevalence and density (mf/20 µl of blood) reductions. In Japan, among various dosage schemes tested by different workers, Sasa (1976) [17] stressed the importance of the size of total dosage given, rather than the schedule of daily, weekly or monthly treatment, and recommended a total dosage of 72 mg/kg at 6 mg/kg daily for 12 days.

The WHO Expert Committee on Filariasis analyzed the accumulated data on DEC dosage and reported in 1967 [18] that "an adequate amount seems to be a total dose of about 72 mg of diethylcarbamazine citrate per kg body weight". Spaced doses of 6 mg/kg once a week or once a month (12 times) were preferred to daily doses to reduce adverse reactions. The next WHO Expert Committee Report (1974) [19] confirmed the same total dose of 72 mg/kg for *W. bancrofti* infections and 30-40 mg/kg for *B. malayi* infections. Daily treatment was considered impractical for mass treatment. In 1984, the 4th Committee Report [20] reiterated the same total dosage for *W. bancrofti*.

b-2. *Effect of low-dose treatments: results from a "minority" group*

Several studies with *W. bancrofti* reported the remarkable effectiveness of DEC at low dosages. Rachou & Scaff (1958) in Brazil (quoted by Hawking, 1962 [21]) reported that only one dose at 6 mg/kg reduced the mf prevalence rate from 100% (pretreatment level) to 62%, and mf density by 91.4% when assessed 12 months after treatment. The authors recommended annual or biannual mass treatments without prior blood tests for mf. In Gambia, McGregor & Gilles (1960) [22] observed that a total dose of 12.5 mg/kg (2.5 mg/kg daily for 5 days) reduced microfilarial load by 90-98% 43 months after treatments and left the noteworthy comment that "mass-treatment campaigns aimed at dosing all inhabitants at spaced intervals (2-4 years) might in the long run prove to be the most effective and economical way." Nearly 2 decades later, in French Polynesia, Laigret et al. (1978) [23] reported that DEC 6 mg/kg (400 mg for males and 300 mg for females) given once per year for 3 years successfully reduced the mf rate from 100% (pretreatment level) to 12% and the average mf density from 15 per 20 µl of blood to 0.3. The annual single-dose treatment was applied to ca. 50,000 people for 4 years and succeeded in reducing the mf prevalence from 4.4% to 1.9%. In practice, not all of the people took 4 doses; the result was obtained with the average of 2.76 doses in 4 years [24].

It is surprising to find that the dosages recommended for DEC treatment differed so widely in range. Understandably, researchers seemed to focus more on the cure of infection in the early stage of dosing trials. Due to the reappearance of mf after treatments, adulticidal effect was considered a key issue in judging the efficacy of a drug. Thus, the necessity of multi-dose treatment with a high total dosage must be stressed. On the other hand, it seems that a small number of researchers, especially those working in less-developed settings, paid more attention to the applicability of a treatment scheme. Also, the experience of difficulty in conducting multi-dose treatments and the recognition of adverse effects in such treatments must have convinced researchers to accept regimens not ideally effective but operationally feasible. The realization that very light infections had been missed previously when conventional blood tests (with 20-60 µl of F-P blood) were used for diagnosis called for a more suitable means of large-scale mass treatment. In 1984, the WHO Expert Committee on Filariasis, for the first time, mentioned the effectiveness of yearly treatments at 6 mg/kg [20].

C. Filariasis control in Samoa and Fiji with annual single-dose MDA using diethylcarbamazine

c-1. *Countries and their filariasis situations*

Samoa, an independent country in the South Pacific, had a population of 160,000 (1990) in the 2 main islands of Upolu and Savaii. Diurnally subperiodic *W. bancrofti*, transmitted by *Aedes polynesiensis* and *Aedes samoanus*, is endemic. The prevalence study in 1965 revealed a mf rate of 19.1% (n = 10,129) by the 20 µl F-P blood smear method. The first nationwide MDA in 1965/66 using DEC (5 mg/kg once a week for 6 weeks, followed by the same dosage once a month for 12 months) reduced the mf rate to 1.63% (n = 42,697) in 1967, and the second MDA in 1971 (6 mg/kg once a month for 12 months) further reduced the rate – assessed by the 60 µl F-P method in 1972 – to 0.24% (n = 6,361). Despite continuing treatment of known mf positives, the prevalence increased gradually, and in 1979, reached 3.8% (n = 8,385) by 60 µl blood smear and 4.5% (n = 8,385) by the nuclepore filtration method using 1 ml of venous blood (1 ml NP method). The situation was alarming, because mf rate (by 1 ml NP method) of adult males aged ≧30 years had already reached the 20% level [25].

Fiji is the largest island country in the region, with a total population of 726,400 (1990) scattered over 100 islands. The two main islands are Viti Levu and Vanua Levu. Diurnally subperiodic type *W. bancrofti*, transmitted by *Ae. polynesiensis*, *Ae. pseudoscutellaris* and several other mosquito species, is endemic. In 1958, the mf prevalence determined by 60 µl F-P method in the delta area of the Rewa River, Viti Levu, was 12.2% (n = 1,200), which decreased

to 2.7% (n = 1,123) in 1959 after 2 rounds of MDA with DEC (400 mg once, 6 times weekly). However, by 1963, the rate increased to a level of 5% [26]. The 1968-69 studies in Taveuni and Koro islands, and Vanua Levu revealed a mf prevalence of 23% (n = 947) and 13% (n = 3,538) by the 60 µl F-P method, respectively (computed from the data by Mataika et al., 1971 [27]). A nationwide MDA campaign was commenced in 1969 using DEC at 5 mg/kg weekly for 6 weeks, followed by 22 monthly treatments (totally 28 doses, 140 mg/kg). The whole country was covered in 5 stages, and the campaign, which reached completion in 1975, successfully reduced the mf prevalence to 1% or less, but subsequent blood surveys suggested a gradual increase in infection [28]. The surveys in 1983-84 in the 2 remote islands of Lau and Rotuma revealed mf rates of 7.9% (n = 2,329) and 21.2% (n = 1,689) by the 60 µl F-P method, respectively [29]. In a 1985 survey in Kadavu island, the mf rate was 6.9% by the same method (n = 4,686) [30].

Table 1. Comparison of the effects of 3 different DEC dosages given as a single dose and assessed 12 months after treatment

	Dosages		
	4 mg/kg	6 mg/kg	8 mg/kg
No. examined (mf carriers)	51	41	45
No. mf negative after treatment	15	22	18
(% cure rate)	(29.4)	(53.7)	(40.0)
Decrease in mf count, expressed as mean of log (mf +1)			
Pre-treatment (A)	2.117	2.003	2.198
Post-treatment (B)	1.384	0.751	1.010
Change	0.733	1.251	1.188
% decrease*	81.5	94.4	93.5

* Calculated as 100 x [antilog (A) - antilog (B)]/antilog (A).
{Source: Partially adopted from Ref. [31]}

c-2. *WHO/Samoa Filariasis Research Project: Confirmation of efficacy of annual single-dose treatment*

In 1976, when the WHO/Samoa Filariasis Research Project started, it had become standard practice in the treatment of bancroftian filariasis to give a total DEC dose of 72 mg/kg in 12 treatments at 6 mg/kg each. However, difficulties in multi-dose treatment had been encountered in many endemic countries. Especially in Samoa, where a year-long multi-dose MDA was conducted twice in 1965/66 and 1971 utilizing limited health resources, the government was reluctant to repeat the procedure. In the midst of this situation, a report from French Polynesia that annually spaced single-dose DEC at 6 mg/kg was effective in reducing mf rate and density [23] brought encouraging news. Although the regimen was not popular in those days, the Research Project in Samoa decided to evaluate the efficacy of DEC single dose 12 months after treatment.

In the study in 1979-81, a single DEC dose of 4 mg/kg, 6 mg/kg or 8 mg/kg was administered to mf positive persons and the change in mf was assessed at 12 months by the 1 ml NP method (Table 1). The cure rate (% mf negative after treatment) was 29.4%, 53.7% and 40.0%, and the % decrease in geometric mean mf count was 81.5%, 94.4% and 93.5%, respectively for 4 mg/kg, 6 mg/kg and 8 mg/kg regimens. There was no significant difference among the cure rates, but the % decrease obtained with 4 mg/kg regimen was less than that of the 6 mg/kg or 8 mg/kg regimen ($P < 0.01$). Side reactions were studied by questioning people between 5 and 15 days after treatment. The occurrence of reactions (all types combined) was significantly higher in the 8 mg/kg regimen (77.9%) than in the other regimens (57-59%). It was concluded that annual single-dose DEC treatment at 6 mg/kg was suitable for the nationwide treatment for filariasis [31]. In 1981, upon completion of the study, the government of Samoa in collaboration with the Western Pacific Regional Office of WHO decided to implement a national MDA program based on this treatment.

c-3. *Nationwide MDA in Samoa with once-a-year treatment: Long-term efficacy*

A national MDA using a single dose of DEC at 6 mg/kg was started in 1981. All Samoans, except infants under the age of 1 year, pregnant women, sick people, and the very old, were the targets. After completion of the census in every village and town in the country with assistance of village Women's Committees, 3 MDAs were carried out under the supervision of medical staff by members of Women's Committees in 1982, 1983, and 1986, with a treatment coverage of 86.3%, 83.8% and 82.6%, respectively. The total population in 1986 was 159,199. The evaluation blood surveys were carried out 4 times, before and after each MDA, using 60 µl blood smears from some 9,600-13,700 people in 26-34 villages on each occasion. The MDAs reduced the mf prevalence gradually from 8.0% to 3.8% (52% reduction) in males, and from 3.2% to 1.3% (59% reduction) in females. The mf densities (geometric mean of positive counts per 60 µl) decreased from 23.1 to 9.1 (61% reduction) in males and from 14.6 to 9.4 (36% reduction) in females. The change in mf prevalence is summarized in Fig. 2, before and after 3 MDAs according to sex and age [32].

The transmission potential or infectivity index (%) of total population (IIT), which is an estimated mosquito in-

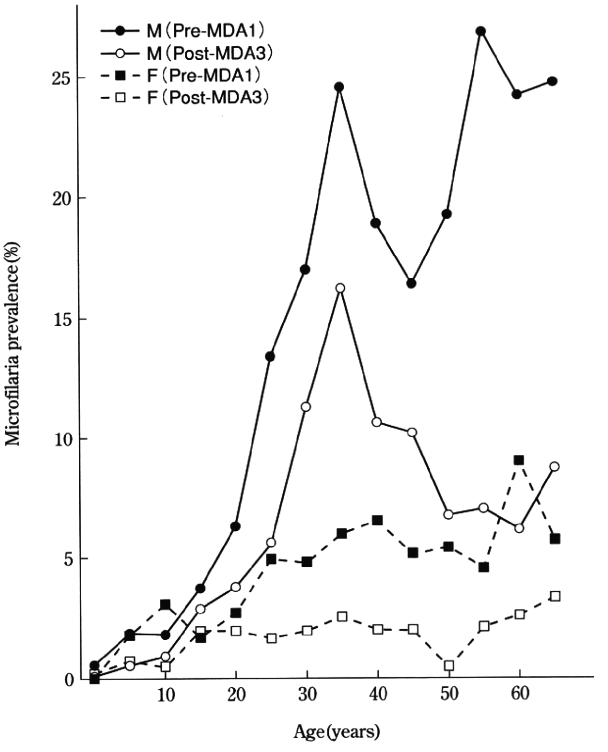

Fig. 2 Change in microfilaria prevalence before and after 3 annual single-dose MDAs with DEC at 6 mg/kg, analyzed by sex and age group (study in Samoa) {Figure redrawn from Ref. [32]}

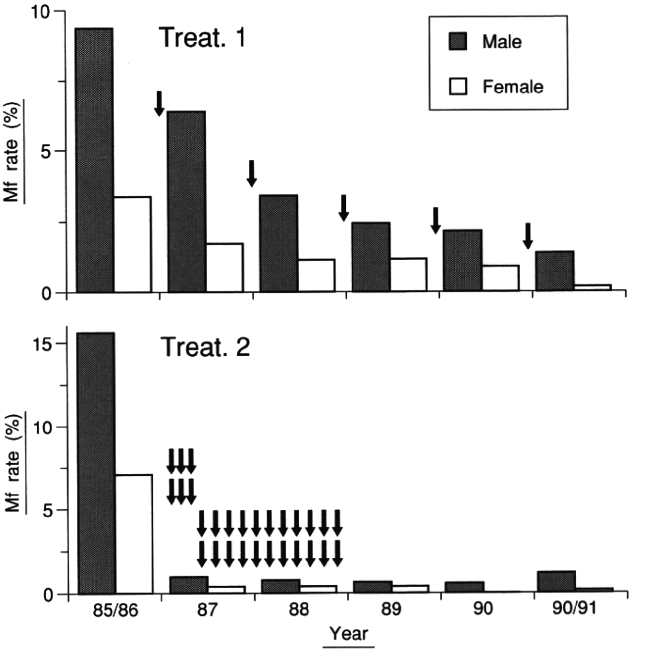

Fig. 3 Comparison of 2 MDA schemes with DEC: 5 rounds of annual single-dose treatment at 6 mg/kg (Treat. 1) and 28-dose treatment at 5 mg/kg given weekly for 6 weeks and monthly for 22 months (Treat. 2). Each arrow indicates a single treatment. {Figure redrawn from Ref. [35]}

fection rate [33], was reduced from 2.18 before MDA to 0.67 (70% reduction) after 3 MDAs. Entomological studies were also conducted at Vailu'utai village on Upolu Island. A total of 1,758 *Ae. polynesiensis* were dissected before MDA and 5,206 after the 2nd MDA. The results revealed a decrease in mosquito infection rate from 0.97% to 0.06% and the infective rate (% of mosquitoes having the infective stage of larvae) from 0.28% to 0.02% [32].

These findings indicated the remarkable long-term efficacy of annually spaced single-dose MDAs, given in fact 3 times in 6 years, and at the same time, the feasibility of a nationwide control program in which people are the major players.

c-4. *Fiji study for confirmation of efficacy of 5 rounds of annual single-dose treatment with DEC: comparison with 28 multi-dose MDA*

Mataika et al. (1993) [34] carried out an extensive study comparing DEC efficacy between 5 annual single-dose MDAs at 6 mg/kg (total 30 mg/kg) and very intensive 28-dose MDA (5 mg/kg once a week for 6 weeks, then monthly for 22 months; total 140 mg/kg). The results are shown in Fig. 3 [35]. The annual scheme reduced the mf rate year by year from 6.5% before treatment (average of males and females) to 0.9% after 5 treatments (87% reduction), while in the multi-dose scheme, the rate dropped sharply from 11.6% to 0.8% in 1987, and to 0.9% at 5 years (93% reduction). However, without treatment for more than 2 years after completion of the intensive 2-year regimen, a slight but significant increase in mf rate was observed in 1990/91 compared with the previous year. This indicates the advantage of continued annual doses rather than a concentrated multi-dose treatment. This study reconfirmed the effectiveness of annual single-dose MDAs. It was obvious that the annual scheme was much easier and more practical than the multi-dose scheme.

D. Low-density microfilaremia in Samoa and its significance in filarial transmission

d-1. *What is low-density microfilaremia?*

There are mf densities that are too low to be detected by conventional blood smears with 20-60 μl of F-P blood. The employment of nuclepore/millipore filtration of 1 ml venous blood has facilitated the detection of low density mf carriers. Low mf density was defined variously by re-